Viscous corrections to electromagnetic emissivities in QCD

Yizhuang Liu[*] and Ismail Zahed[†]

Department of Physics and Astronomy, Stony Brook University, Stony Brook, New York 11794-3800, USA
(Received 13 September 2017; published 28 December 2017)

We provide a general framework for the derivation of the hydrodynamical corrections to the QCD electromagnetic emissivities in a viscous fluid. Assuming that the emission times are short in comparison to the fluid evolution time, we show that the leading corrections in the fluid gradients are controlled by the bulk and shear tensors times pertinent response functions involving the energy-momentum tensor. In a hadronic fluid phase, we detail these contributions using spectral functions. Using the vector dominance approximation, we show that the bulk viscosity correction to the photon rate is sizable, while the shear viscosity is negligible for about all frequencies. In the partonic phase near the transition temperature, we provide an assessment of the viscous corrections to the photon and dilepton emissions, using a nonperturbative quark-gluon plasma with soft thermal gluonic corrections in the form of operators of leading mass dimension. Again, the thermal bulk viscosity corrections are found to be larger than the thermal shear viscosity corrections at all energies for both the photon and dilepton in the partonic phase.

I. INTRODUCTION

One of the major achievements of the heavy ion program at the Relativistic Heavy Ion Collider and now also at the LHC is the emergence of a new state of matter under extreme conditions, the strongly coupled quark gluon plasma (sQGP) with near-ideal liquid properties [1–6]. The prompt release of a large entropy in the early partonic phase together with a rapid thermalization and short mean free paths points to a partonic fluid. The anisotropies of the produced hadrons and photons suggest a near-ideal fluid [7–13].

Small deviations from the ideal limit appear to follow from dissipative effects, suggesting that the shear viscosity of the sQGP fluid is very close to its quantum bound [14]. However, this interpretation requires some care since the emitted hadrons interact strongly throughout the fluid history and particularly in the late stages of the evolution composed essentially of a fluid of hadrons. In contrast, the emitted photons or dileptons are continuously emitted throughout the evolution of the fluid without secondary interactions. They provide for an alternative probe of the nature and strength of these viscous corrections.

So far, most of the hydrodynamical corrections to the electromagnetic emissivities have made use of weakly coupled kinetic theory to modify the phase space distributions of either partons or hadrons in $2 \rightarrow 2$ rate processes [15]. Holographic calculations for the electromagnetic emissivities for $\mathcal{N} = 4$ supersymmetry (SUSY) were carried in near equilibrium in Ref. [16] and far from equilibrium in Ref. [17]. In light of this, it is important to seek a full nonperturbative analysis of the electromagnetic emissivities in a viscous QCD fluid that relies solely on a near-equilibrium approximation and a fluid gradient expansion.

The purpose of this paper is to provide such a framework for the analysis of the emission of photons and dileptons from a nonideal hydrodynamical QCD fluid that does not rely on perturbation theory. Assuming that the electromagnetic emission time is shorter than the fluid unfolding time, we show how to organize the rates in the near-equilibrium phase by expanding in the fluid derivatives. The emerging fluid bulk and shear tensors are multiplied by pertinent correlation functions involving the energy-momentum tensor in equilibrium.

The organization of the paper is as follows. In Sec. II, we show how to assess the electromagnetic emissivities in a fluid near equilibrium by capturing the slow fluid flow in a density matrix. In Sec. III, we show that in leading order in the fluid gradients the electromagnetic emissivities receive contributions proportional to the bulk and shear tensors times Kubo-like response functions involving the energy-momentum tensor. In Sec. IV, we analyze the leading viscous corrections to the electromagnetic emissivities in the hadronic phase, and in Sec. V, we analyze them in a nonperturbative partonic phase. Our conclusions are in Sec. VI. A background field analysis for the soft gluon corrections in the partonic phase is outlined in Appendix A. We also detail the leading contribution to the photon thermal viscous corrections in Appendix B.

II. PHOTON EMISSION IN A FLUID

In thermal equilibrium, the photon emission rate is fixed by the Wightman function for the electromagnetic current [18]

$$\frac{d\Gamma_0}{d^3 k} = -\frac{\alpha g^{\mu\nu}}{4\pi^2 |k|} \langle \mathbb{G}_{\mu\nu}^<(q) \rangle_0 \qquad (1)$$

with

[*]yizhuang.liu@stonybrook.edu
[†]ismail.zahed@stonybrook.edu

$$\mathbb{G}_{\mu\nu}^{<}(q) = \int d^4x e^{-iq\cdot x} J_\mu(0) J_\nu(x). \qquad (2)$$

The averaging is carried over the state of maximum entropy or equivalently a thermal distribution of fixed temperature $1/\beta$. In writing (2), space-time translational invariance is assumed. Most studies of photon emission at collider energies have relied on (1), with some recent exceptions using modifications based on kinetic theory.

For a system far out of equilibrium, its evolution and emission rates are convoluted. However, for large times, the system nears equilibrium, and its evolution follows the lore of hydrodynamics. In this regime, the microscopic electromagnetic emission rates can be assumed to occur on time scales shorter than the times it takes for the fluid to flow. In this decoupling approximation, we may ask for the changes caused by a fluid velocity profile on the electromagnetic emissivities of a QCD fluid, for instance.

With this in mind, we may still rely on (2) at any time $\bar{t}$ since space-time microscopic translational invariance holds. Now, consider the emission on a fluid timelike surface defined by $\bar{t} = $ constant, and canonically quantize the field theory on this surface. Let $\phi_{\bar{t}}$ be a generic operator on this surface. Its time evolution proceeds through

$$\phi_{\bar{t}}(t,\vec{x}) \equiv \phi(\bar{t}+t,\vec{x}) = e^{iHt}\phi(\bar{t},\vec{x})e^{-iHt} \qquad (3)$$

with the canonical Hamiltonian $H = H[\phi_{\bar{t}}, \pi_{\bar{t}}]$. The emission on this timelike surface is still controlled by the general Wightman function

$$\langle \mathbb{G}_{\bar{t}\mu\nu}^{<}(t,\vec{x}) \rangle = \mathrm{Tr}(\rho(\bar{t}_0)J_{\bar{t}\mu}(0,\vec{0})J_{\bar{t}\nu}(t,\vec{x})) \qquad (4)$$

with an initial density operator at $\bar{t}_0 < \bar{t}$. For a state in equilibrium, we have

$$\rho(\bar{t}_0) \to \rho(\bar{t}) = e^{-\beta_{\bar{t}}(H-F_{\bar{t}})}. \qquad (5)$$

However, for a state near equilibrium, we define

$$\rho(\bar{t}_0) = \rho(\bar{t})U(\bar{t},\bar{t}_0) \equiv \rho(\bar{t})T_\tau e^{\int_0^1 d\tau\Sigma(\bar{t}-i\beta_{\bar{t}}\tau,\bar{t}_0)}. \qquad (6)$$

T_τ is the ordering along the τ line. The operator Σ is a measure of the entropy change from $\bar{t}_0 \to \bar{t}$ as discussed in Ref. [19]. For our case, it is sufficient to note that it follows from the response to the insertion of $\int d^4x \partial_i\beta_j T_{ij}$,

$$\Sigma(\bar{t}-i\beta\tau,\bar{t}_0) = \partial_i\beta_j \int_{\bar{t}_0}^{\bar{t}} dt' \int_0^1 d\tau d^3x' T_{ij}(\vec{x}', t' - i\tau\beta_{\bar{t}}), \qquad (7)$$

for a time-independent but spatially dependent fluid velocity β_i. We note that (6) can be equally defined through

$$\rho(\bar{t}_0) = \tilde{U}(\bar{t},\bar{t}_0)\rho(\bar{t}) \equiv T_\tau^\star e^{\int_0^1 d\tau\Sigma(\bar{t}+i\beta_{\bar{t}}\tau,\bar{t}_0)}\rho(\bar{t}). \qquad (8)$$

For $\bar{t} \gg \bar{t}_0$, the averaging over $\rho(\bar{t}_0)$ asymptotes the equilibrium average captured by $\rho(\bar{t})$, modulo derivative corrections due to the fluid gradients as captured in Σ. In what will follow, we will set $\beta = \beta_{\bar{t}}$ for notational simplicity.

III. GRADIENT EXPANSION

For a baryon free fluid flow characterized locally by β_i, we can now organize (4) using an expansion in fluid gradients $\partial_i\beta_j$. For a given time $\bar{t}$, the leading contribution emerges only by keeping $\rho(\bar{t})$ in (6). In this order, Eq. (4) yields (1) in equilibrium. The fluid gradient corrections appear at next-to-leading order by expanding the τ-ordered exponent and retaining only the first gradient correction in Σ,

$$\rho(\bar{t}_0) \approx \rho(\bar{t})\left(1 - \partial_i\beta_j \int_{\bar{t}_0}^{\bar{t}} dt' \int_0^1 d\tau d^3x' T_{ij}(\vec{x}', t' - i\tau\beta)\right)$$

$$\approx \left(1 - \partial_i\beta_j \int_{\bar{t}_0}^{\bar{t}} dt' \int_0^1 d\tau d^3x' T_{ij}(\vec{x}', t' + i\tau\beta)\right)\rho(\bar{t}). \qquad (9)$$

Inserting (9) in (4) yields the first-order fluid gradient correction to the electromagnetic emissivities

$$\begin{aligned}\langle \mathbb{G}_{\bar{t}\mu\nu}^{<}(t,\vec{x}) \rangle_1 &\approx -\int_{\bar{t}_0}^{\bar{t}} dt' \int_0^1 d\tau \langle T_{ii}(t' - i\tau\beta, \vec{q}=0)\\ &\times J_{\bar{t}\mu}(0)J_{\bar{t}\nu}(x)\rangle_\beta \theta\\ &- \int_{\bar{t}_0}^{\bar{t}} dt' \int_0^1 d\tau \langle T_{ij}(t' - i\tau\beta, \vec{q}=0)\\ &\times J_{\bar{t}\mu}(0)J_{\bar{t}\nu}(x)\rangle_\beta \sigma_{ij}\end{aligned} \qquad (10)$$

with $\theta = \partial_m\beta_m/3$. The transverse and traceless shear velocity tensor is defined as

$$\sigma_{ij} = \frac{1}{2}\left(\partial_i\beta_j + \partial_j\beta_i - \frac{2}{3}\delta_{ij}\partial_m\beta_m\right). \qquad (11)$$

Equation (10) involves the causal change in the electromagnetic emissivity caused by the fluid bulk and shear parts of the energy-momentum tensor T_{ij}, while evolving from $\bar{t}_0 \to \bar{t}$.

The Kubo-like three-point response function in (10) can be made more explicit by defining

$$O_{ij}^{\pm} = \int_{\bar{t}_0}^{\bar{t}} dt' \int_0^1 d\tau \int d^3x' T_{ij}(t' \mp i\tau\beta, \vec{x}') \qquad (12)$$

so that

$$\left\langle \mathbb{G}^<_{\bar{\imath}\mu\nu}(t,\vec{x}) \right\rangle_1 \approx -\langle O^-_{\bar{\imath}i} J_{\bar{\imath}\mu}(0) J_{\bar{\imath}\nu}(x)\rangle\theta - \langle O^-_{\bar{\imath}j} J_{\bar{\imath}\mu}(0) J_{\bar{\imath}\nu}(x)\rangle\sigma_{ij}.$$

$$(13)$$

The equivalence between the left-right decomposition in (9) suggests that the operator $O^\pm_{ij}$ commutes with the Hamiltonian. Indeed, we have

$$[H, O^\pm_{ij}] = -i \int_{\bar{t}_0}^{\bar{t}} dt' \int_0^1 d\tau \int d^3x' \partial_{t'} T_{ij}(t' \mp i\tau\beta, \vec{x}')$$

$$= \pm \frac{1}{\beta} \int_{\bar{t}_0}^{\bar{t}} dt' d^3x' (T_{ij}(t \mp i\beta, \vec{x}) - T_{ij}(t, x')). \quad (14)$$

If the decorrelation time in the Kubo-like result (13) is short in comparison to the fluid evolution time, we may regard $t_H = \bar{t} - \bar{t}_0$ as large. This will be understood throughout. Therefore, the commutator in (14) vanishes modulo asymptotic terms. We note that the operator O_{ij} is related to the time integration of the first moment of the momentum density, which is conserved,

$$\partial_t \int d^3x (x_i T^0_j(t, \vec{x})) = \int d^3x (x_i \partial_t T^0_j(t, \vec{x}))$$

$$= -\int d^3x (x_i \partial_k T^k_j(t, \vec{x}))$$

$$= \int d^3x T_{ij}(t, \vec{x}). \quad (15)$$

It follows that its expectation value is proportional to the time length t_H characteristic of the hydrodynamical evolution, which is assumed to be much larger than the characteristic time for electromagnetic emission. This point will become clear in the explicit calculations to follow.

IV. HADRONIC PHASE

In a QCD fluid, the analysis of the response functions depends on the nature of the underlying phase. At low temperatures, the fluid is mostly hadronic, while at high temperature, it is partonic but strongly coupled near the crossover temperature. In the hadronic phase with zero baryon density and no strangeness, Eq. (13) can be organized by expanding it in increasing densities of the lightest stable thermal hadrons, i.e., pions following similar analyses for the equilibrium rates in Ref. [20]. Specifically, we have

$$G^<_{\bar{\imath}ij}(x) = \text{Tr}(e^{-\beta(H-F)} O^\pm_{ij}(J(\bar{x})J(\bar{x}-x)))$$

$$= G^<_{ij,0\pi} + \int (d\tilde{\pi}_1)_{ij} G^<_{1\pi} + \frac{1}{2!} \int (d\tilde{\pi}_1 d\tilde{\pi}_2)_{ij} G^<_{2\pi} + \cdots,$$

$$(16)$$

where we have defined the unordered and connected matrix elements

$$G^<_{n\pi}(x)$$
$$= \langle \pi^{a_1}(k_1)...\pi^{a_n}(k_n)|J(\bar{x})J(\bar{x}-x)|\pi^{a_1}(k_1)...\pi^{a_n}(k_n)\rangle$$

$$(17)$$

with the pion thermal phase space factors $(E_i^2 = \vec{k}_i^2 + m_\pi^2)$

$$(d\tilde{\pi}_1)_{ij} = \frac{d^3k_i}{(2\pi)^3}\frac{t_H}{2E_i}\frac{k_i k_j}{E_i} n_B(E_i)(1 + n_B(E_i)) \quad (18)$$

and the identification $t_H = 2\pi\delta(0_E)$. This can be justified by explicitly performing the trace using the in states. For instance, for the one-pion connected pieces, we have

$$\sum_{n,[k]} \langle \pi(k_1)...\pi(k_n)|e^{-\beta H} O^\pm_{ij} JJ|\pi(k_1)...\pi(k_n)\rangle$$

$$= \sum_{n_2,k_2,...}\cdots\sum_{n_1,k_1} \frac{n_1^2}{n_1} \langle \pi(k_1)|JJ|\pi(k_1)\rangle e^{-n_1\beta E_{k_1}} \frac{k_{1i}k_{2j}}{E_1}$$

$$= e^{-\beta F_0} \int \frac{d^3k}{(2\pi)^3}\frac{t_H}{2E_k}\frac{k_i k_j}{E_k} n_B(1+n_B)\langle \pi(k)|JJ|\pi(k)\rangle.$$

$$(19)$$

When comparing the viscous corrected hadronic contributions in (16) and (17) to the uncorrected ones, the difference is in the insertion of the operator $O^\pm_{ij}$ over the external pion in states. $O^\pm_{ij}$ is essentially the energy-momentum tensor, which, once inserted, amounts to a change in the one-pion phase space

$$\frac{d^3k}{(2\pi)^3}\frac{1}{2E_k} \rightarrow \frac{d^3k}{(2\pi)^3}\frac{1}{2E_k}\frac{t_H k_i k_j}{E_k}.$$

These are essentially the corrections induced by the viscosity on the hadronic emissivities which are still captured by the hadronic matrix elements $\langle n\pi|JJ|n\pi\rangle$. For $\beta t_H \sim 1$ and $\beta \sim 1/m_\pi$, these corrections are of order $t_H kk/E_k \sim 1/\sqrt{2}$. A more quantitative assessment of these corrections will be given below.

A. $G^<_{ij,0\pi}$ contribution

The contributions to $G^<_{ij,0\pi}$ in (16) follow from $2\pi, 4\pi, ...$ insertions in the intermediate state and are all found to vanish. Indeed, consider the leading 2π insertion to $G^<_{ij,0\pi}$,

$$G^<_{ij,0\pi}(x) = \langle 0|O^\pm_{ij} J(\bar{x})J(\bar{x}-x)|0\rangle$$

$$\approx 2\int \frac{d^3k_1 d^3k_2}{(2\pi)^6 2E_{k_1} 2E_{k_2}} \langle 0|O^\pm_{ij}|\pi^+(k_1)\pi^-(k_2)\rangle$$

$$\times \langle \pi^+(k_1)\pi^-(k_2)|J(\bar{x})J(\bar{x}-x)|0\rangle, \quad (20)$$

where the overall factor 2 accounts for the two charged pions. The covariantized transition matrix element in (20) in leading order in the pion momentum reads

$$\langle 0|T_{\mu\nu}(t,x)|\pi^+(k_1)\pi^-(k_2)\rangle$$
$$= e^{-it(E_1+E_2)+i\vec{x}\cdot(\vec{k}_1+\vec{k}_2)}$$
$$\times (-k_{1\mu}k_{2\nu} - k_{2\mu}k_{1\nu} - g_{\mu\nu}(-k_1 \cdot k_2 - m_\pi^2)). \quad (21)$$

At asymptotic times or large t as required by the out-field condition, this contribution vanishes, owing to the non-vanishing Fourier component in time. This result is consistent with the fact that O_{mn} connects only states with $E_m = E_n$. Clearly, this result carries to all $2n\pi$ insertions, making $G_{ij,0\pi}^< = 0$.

B. $G_{1\pi}^<$ contribution

The leading correction to (13) arises from the thermal one-pion contribution to $G_{1\pi}^<$. Specifically, we have

$$(d\tilde{\pi}_1)_{ij}G_{1\pi}^<(x) = \frac{d^3k_1}{(2\pi)^3}\frac{t_H}{2E_1}\frac{k_{1i}k_{1j}}{E_1}n_B(1+n_B)$$
$$\times \langle \pi^a(k_1)|J(\bar{x})J(\bar{x}-x)|\pi^a(k_1)\rangle, \quad (22)$$

which is seen to involve part of the forward photon-pion scattering amplitude. Its explicit form follows from the general strictures of broken chiral symmetry, crossing symmetry, and unitarity [20,21],

$$(d\tilde{\pi}_1)_{ij}G_{1\pi}^<(q) = \frac{d^3k_1}{(2\pi)^3}\frac{t_H}{2E_1}\frac{k_{1i}k_{1j}}{E_1}n_B(1+n_B)$$
$$\times \left(-\frac{6}{f_\pi^2}(k_1-q)^2\mathrm{Im}\mathbf{\Pi}_A((k_1-q)^2)\right). \quad (23)$$

Here, Π_A is the AA correlation function of the axial-vector current in the vacuum [20]. Its spectral form follows from τ-decay measurements into an odd number of pions. The result (23) grows linearly with the hydrodynamical time t_H, that is, the time it takes the externally applied hydrodynamical gradient $\partial_i\beta_j$ to change. This time is proportional to the transport mean free path $t_H \approx \lambda_{\mathrm{mfp}}$, which in turn is determined by the viscosities,

$$t_H \to t_\eta \approx \frac{\eta}{e+p} \quad \text{shear}$$
$$t_H \to t_\zeta \approx \frac{\zeta}{e+p} \quad \text{bulk.} \quad (24)$$

Here, η and ζ are the shear and bulk viscosities, respectively, and e and p are the energy and pressure densities, respectively. These hydrodynamical times will be understood in the results to follow.

The higher-order corrections $G_{2\pi}^<, \dots$ in (16) are suppressed by additional viscous phase space factors:

$$\int \frac{d^3k}{(2\pi)^3}\frac{t_H}{2E_k}\frac{kk}{E_k}n_B \sim \frac{\beta t_H}{\sqrt{2}}\int \frac{d^3k}{(2\pi)^3}\frac{n_B}{2E_k} = \kappa_\pi\frac{\beta t_H}{\sqrt{2}}.$$

It is readily checked that in the range of temperatures $0 < 1/(\beta m_\pi) < 1$ the effective number of pions κ_π remains small with $0 < \kappa_\pi < 1/2$.

C. Viscous photon rate

The viscous corrections to the photon rates due to a baryon free fluid of hadrons follow from the results in (1)–(13) and in (16)–(23). Specifically, if we insert (23) into (1), we obtain

$$\frac{d\Gamma_1^<}{d^3k} = \frac{\alpha t_H}{2\pi^2\omega}\int \frac{d^3p}{(2\pi)^3}\frac{1}{2E}\frac{e^{\beta E}}{(e^{\beta E}-1)^2}\frac{p^2}{E}$$
$$\times (2\partial_i\beta_j\mathbf{P}_{ij}\cos^2\theta_p + \partial_i\beta_j\mathbf{N}_{ij}\sin^2\theta_p)$$
$$\times \left(\frac{3}{f_\pi^2}(p-k)^2\mathrm{Im}\mathbf{\Pi}_A((p-k)^2)\right) \quad (25)$$

with $\mathbf{P}_{ij} = \hat{k}_i\hat{k}_j$ and $\mathbf{N}_{ij} = \delta_{ij} - \hat{k}_i\hat{k}_j$, after making use of the identity

$$\int d^3p\,\hat{p}_i\hat{p}_j F(p,k)$$
$$= 2\mathbf{P}_{ij}\int d^3p\cos^2\theta_p F(p,k) + \mathbf{N}_{ij}\int d^3p\sin^2\theta_p F(p,k).$$

Now, we define the bulk parameter $\theta = \partial_m\beta_m/3$ and the shear parameter $\sigma = \sigma_{ij}\hat{k}_i\hat{k}_j$ and rewrite

$$2\partial_i\beta_j\mathbf{P}_{ij}\cos^2\theta_p + \partial_i\beta_j\mathbf{N}_{ij}\sin^2\theta_p = \sigma(3\cos^2\theta_p - 1) + 2\theta, \quad (26)$$

in terms of which (25) reads

$$\frac{d\Gamma_1^<}{d^3k} = -\frac{\alpha}{2\pi^2\omega}\int \frac{d^3p}{(2\pi)^3}\frac{1}{2E}\frac{e^{\beta E}}{(e^{\beta E}-1)^2}\frac{p^2}{E}$$
$$\times (t_\eta\sigma(3\cos^2\theta_p - 1) + 2t_\zeta\theta)$$
$$\times \left(-\frac{3}{f_\pi^2}(p-k)^2\mathrm{Im}\mathbf{\Pi}_A((p-k)^2)\right) \quad (27)$$

after using the substitution (24).

For comparison, the equilibrium photon rates (1) in the hadronic phase can also be calculated using the Wightman function with the result

$$\frac{d\Gamma_0^<}{d^3k} = \frac{\alpha}{\pi^2\omega}\int \frac{d^3p}{(2\pi)^3}\frac{1}{2E}\frac{1}{e^{\beta E}-1}$$
$$\times \left(\frac{3}{f_\pi^2}(p-k)^2\mathrm{Im}\mathbf{\Pi}_A((p-k)^2)\right). \quad (28)$$

However, Eq. (28) to this order does not enforce the Kubo-Martin-Schwinger (KMS) condition,

$$G^<(q) = \frac{2}{e^{\beta q_0} + 1} \mathrm{Im}\, iG^F(q),$$
(29)

which reflects on the causal character of the emissivities. To enforce this condition requires resumming higher-order contributions from the expansion in (16). This is possible, and the result is [20]

$$\frac{d\Gamma_0}{d^3k} = \frac{1}{e^{\beta\omega} + 1} \frac{\alpha}{\pi^2 \omega} \int \frac{d^3p}{(2\pi)^3} \frac{1}{2E} \frac{1}{e^{\beta E} - 1}$$
$$\times \left(\frac{3}{f_\pi^2} (p+k)^2 \mathrm{Im}\Pi_A((p+k)^2) + (k \to -k) \right).$$
(30)

The chief outcomes of this resummation are twofold: a) the appearance of an overall factor of $1/(e^{\beta\omega} + 1)$ and b) a crossing of the spectral function in the integrand that yields the full forward $\gamma^*\pi \to \gamma^*\pi$ Feynman amplitude. We now apply these observations to (27) to obtain

$$\frac{d\Gamma_1}{d^3k} = -\frac{1}{e^{\beta\omega} + 1} \frac{\alpha}{2\pi^2 \omega} \int \frac{d^3p}{(2\pi)^3} \frac{1}{2E} \frac{e^{\beta E}}{(e^{\beta E} - 1)^2} \frac{p^2}{E}$$
$$\times (t_\eta \sigma (3\cos^2\theta_p - 1) + 2t_\zeta \theta)$$
$$\times \left(-\frac{3}{f_\pi^2} (p-k)^2 \mathrm{Im}\Pi_A((p-k)^2) + (k \to -k) \right).$$
(31)

Equation (31) is our final result for the leading viscous correction to the hadronic rate using spectral functions. The total viscous photon hadronic rate follows from (30) plus (31) as

$$\frac{d\Gamma}{d^3k} = \frac{d\Gamma_0}{d^3k} + \frac{d\Gamma_1}{d^3k}.$$
(32)

D. Vector dominance

For a simple estimate of the size of the viscous corrections, we will use the unsummed rates $\Gamma^<_{0,1}$ and make use of the vector dominance model (VDM) to saturate $\mathrm{Im}\Pi_A$. Specifically, we set

$$\mathrm{Im}\Pi_A(s) \approx f_A^2 \frac{\frac{\Gamma}{2}}{(s - m_A^2)^2 + \frac{\Gamma^2}{4}}$$
(33)

with the axial constant $f_A \approx f_\pi$. Here, m_A and Γ are the mass and width of the axial-meson $a1$, with typically $m_A = 1230$ MeV and $\Gamma = 250$ MeV. Inserting (33) in (27) yields the VDM result for the (unsummed) viscous photon rate

$$\frac{d\Gamma_1^<}{d^3k} \approx -\frac{3\alpha}{8\pi^4} \frac{f_A^2}{f_\pi^2} \Gamma \int \frac{p^4 dp\, d\cos\theta_p}{E^2} \frac{e^{\beta E}}{(e^{\beta E} - 1)^2}$$
$$\times \left(\left(t_\zeta \theta - \frac{1}{2} t_\eta \sigma \right) + \frac{3}{2} t_\eta \sigma \cos^2\theta_p \right)$$
$$\times \frac{E - p\cos\theta_p}{(m_A^2 + 2E\omega - 2p\omega\cos\theta_p)^2 + \frac{\Gamma^2}{4}}.$$
(34)

Equation (34) simplifies further as $\beta m_\pi \to 0$ (chiral limit),

$$\frac{d\Gamma_1^<}{d^3k} \approx -\frac{3\alpha}{8\pi^4} \frac{f_A^2}{f_\pi^2} \Gamma \int_{m_\pi}^{\infty} E^3 dE \frac{e^{\beta E}}{(e^{\beta E} - 1)^2}$$
$$\times \left(\left(t_\zeta \theta - \frac{1}{2} t_\eta \sigma \right) f_1(E) + \frac{3}{2} t_\eta \sigma f_2(E) \right),$$
(35)

where we have kept m_π as an infrared regulator in the integration, with

$$f_1(E) = \int_{-1}^{1} dx \frac{1 - x}{(m_A^2 + 2E\omega(1-x))^2 + \frac{\Gamma^2}{4}}$$
$$f_2(E) = \int_{-1}^{1} dx \frac{x^2(1 - x)}{(m_A^2 + 2E\omega(1-x))^2 + \frac{\Gamma^2}{4}}.$$
(36)

Equation (34) is seen to vanish for zero width Γ. To leading order in Γ, Eq. (36) simplifies

$$m_A^4 f_1(E) \approx f_1(x) = \frac{1}{4x^2} \left(\ln(1 + 4x) - \frac{4x}{1 + 4x} \right)$$

$$m_A^4 f_2(E) \approx f_2(x) = \frac{1}{16x^4} \left((3 + 2x)(1 + 2x) \ln(1 + 4x) \right.$$
$$\left. - 8x(1 + x) - \frac{4x(1 + 2x)^2}{1 + 4x} \right)$$
(37)

with $x = E\omega/m_A^2$. Changing the integration variable to x in (34) gives

$$\frac{d\Gamma_1^<}{d^3k} \approx -\frac{3\alpha}{16\pi^4} \frac{f_A^2 m_A^4}{f_\pi^2 \omega^4} \Gamma \int_{\frac{m_\pi \omega}{m_A^2}}^{\infty} dx \frac{x^3 e^{\frac{\beta m_A^2 x}{\omega}}}{(e^{\frac{\beta m_A^2 x}{\omega}} - 1)^2}$$
$$\times (2t_\zeta \theta f_1(x) + t_\eta \sigma (3f_2(x) - f_1(x))).$$
(38)

For comparison, the (unsummed) equilibrium VDM rate (28) in the same approximation reads

$$\frac{d^3\tilde{\Gamma}_0^<}{d^3k} \approx \frac{3\alpha}{8\pi^4} \frac{f_A^2 m_A^2}{f_\pi^2 \omega^3} \Gamma \int_{\frac{m_\pi \omega}{m_A^2}}^{\infty} dx \frac{x^2 f_1(x)}{e^{\frac{\beta m_A^2 x}{\omega}} - 1},$$
(39)

where the lower bound stems from

$$(p+k)^2 = 2E\omega(1 - \cos\theta_p) = m_A^2.$$
(40)

The ratio of the (unsummed) viscous rate (35) to the equilibrium rate (39) takes the simple form

$$
\frac{d\Gamma_1^<}{d\Gamma_0^<} \approx -\frac{m_A^2}{2\omega} \left(\int_{\frac{m_\pi \omega}{m_A^2}}^\infty dx \frac{x^2 f_1(x)}{e^{\frac{\beta m_A^2 x}{\omega}} - 1} \right)^{-1}
$$
$$
\times \left(2t_\zeta \theta \int_{\frac{m_\pi \omega}{m_A^2}}^\infty dx \frac{x^3 e^{\frac{\beta m_A^2 x}{\omega}}}{(e^{\frac{\beta m_A^2 x}{\omega}} - 1)^2} f_1(x) \right.
$$
$$
\left. + t_\eta \sigma \int_{\frac{m_\pi \omega}{m_A^2}}^\infty dx \frac{x^3 e^{\frac{\beta m_A^2 x}{\omega}}}{(e^{\frac{\beta m_A^2 x}{\omega}} - 1)^2} (3f_2(x) - f_1(x)) \right). \quad (41)
$$

In Fig. 1, we show the bulk contribution R_ζ in (41) as the solid-blue curve and the shear contribution R_η in (41) as the orange-dashed curve over a range of frequencies ω in GeV for a temperature $1/\beta = m_\pi$. We have set the shear and bulk factors to $\theta = \sigma = 1$ and fixed the relaxation times to $t_\eta = t_\zeta = \beta$. The smallness of the shear contribution stems from the near cancellation of the $3f_2 - f_1$ in the integrand of (41). The bulk contribution dwarfs the shear contribution in the VDM approximation for about all frequencies. The bulk contribution is also opposite in sign to the shear contribution in leading order. At currently available collider energies, a typical AA collision triggers a hadronic fluid with a size $L \approx 10$ fm. For temperatures $T \approx 200$ MeV, that results in fluid gradients of the size $\theta \approx \sigma \approx 1/TL \approx 1/10$. When combined with the result shown in Fig. 1, this estimate shows that the bulk viscosity correction to the hadronic rate is about 30% across all frequencies, while the shear viscosity correction is negligible. Overall, the bulk hydrodynamical correction appears sizable even in the late stage of the hadronic evolution with small gradients in the form of a small $\theta = \partial_i \beta_i / 3$. These observations deserve to be further checked in current hydrodynamical assessments of the electromagnetic emissivities and without the VDM approximation through the use of the full axial spectral weight.
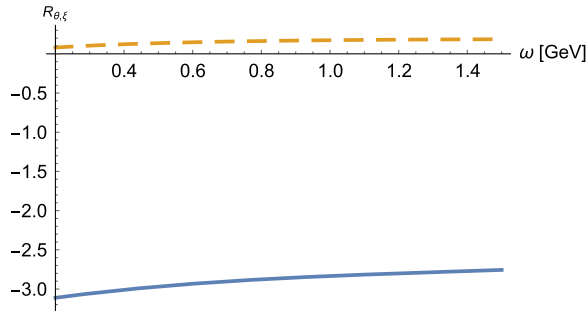

FIG. 1. Ratio (41) for the bulk hadron contribution R_ζ (blue-solid curve) vs ω and for the hadron shear contribution R_η (orange-dashed curve) vs ω in the VDM approximation, for $\beta = 1/m_\pi$, and equal relaxation times $t_\zeta = t_\eta = \beta$ for fixed $\theta = \sigma = 1$.

E. Viscous dilepton rate

The previous results extend to the dilepton rates as well if we recall that for dilepton emissivities Eq. (1) needs to be changed to

$$
\frac{d\mathbb{R}_0}{d^4 q} = -\frac{\alpha^2 \mathbb{B} g^{\mu\nu}}{6\pi^3 q^2} \langle \mathbb{G}_{\mu\nu}^<(q) \rangle_0 \quad (42)
$$

with the leptonic factor

$$
\mathbb{B} = \left(1 + \frac{2m_l^2}{q^2} \right) \left(1 - \frac{4m_l^2}{q^2} \right)^{\frac{1}{2}} \quad (43)
$$

with the threshold $q^2 > 4m_l^2$ and typically $l = e, \mu$. The equilibrium contributions to (42) in the hadronic phase have been discussed in detail using spectral functions in Ref. [22] and hadronic processes in Ref. [23]. From the spectral functions analysis, the result is [22]

$$
\frac{d\mathbb{R}_0}{d^4 q} = -\frac{\alpha^2}{6\pi^3} \frac{\mathbb{B}}{q^2} \frac{2}{e^{\beta\omega} + 1}
$$
$$
\times \left(-3q^2 \text{Im}\Pi_V(q^2) + \int \frac{d^3 p}{(2\pi)^3} \frac{1}{2E} \frac{1}{e^{\beta E} - 1} \right.
$$
$$
\times \left(\frac{12}{f_\pi^2} q^2 \text{Im}\Pi_V(q^2) \right.
$$
$$
- \frac{6}{f_\pi^2} (p - q)^2 \text{Im}\Pi_A((p - q)^2 + q \to -q)
$$
$$
+ \frac{8}{f_\pi^2} ((p \cdot q)^2 - m_\pi^2 q^2) \text{Im}\Pi_V(q^2) \times \text{Re}\Delta_R(p - q)
$$
$$
\left. \left. + q \to -q \right) \right). \quad (44)
$$

The nonequilibrium viscous correction in the hadronic phase follows a similar reasoning as that given for the photons. A rerun of the preceding reasoning shows that $G_{ij,0\pi}^<$ also vanishes in this case. However, $G_{1\pi}^<$ does not, and the result is

$$
(d\pi)_{ij} G_{1\pi}^<(q, k)
$$
$$
= \int \frac{d^3 k}{(2\pi)^3} \frac{t_H}{2E} \left(\frac{k_i k_j}{E_k} \right) n_B (1 + n_B) \left(\frac{12}{f_\pi^2} q^2 \text{Im}\Pi_V(q^2) \right.
$$
$$
- \frac{6}{f_\pi^2} \left(k - q \right)^2 \text{Im}\Pi_A((k - q)^2)
$$
$$
\left. + \frac{8}{f_\pi^2} ((k \cdot q)^2 - m_\pi^2 q^2) \text{Im}\Pi_V(q^2) \times \text{Re}\Delta_R(k - q) \right). \quad (45)
$$

Here, Π_V is the VV correlation of the vector current in the vacuum, and Δ_R is the retarded pion propagator [20]. The spectral form of Π_V follows from $e^+ e^-$ annihilation. The last bracket in (45) is only the *crossed* $\gamma^* \pi \to \gamma^* \pi$

scattering amplitude $\mathcal{T}_{\gamma^*\pi}$, which is seen to reduce to (23) at the photon point or $q^2 = 0$. In terms of (45), the resummed viscous corrections to the dilepton emissivities in a hadronic fluid take the following final form:

$$
\frac{d\mathbb{R}_1}{d^4q} = -\frac{4\alpha^2}{3\pi^2}\frac{\mathbb{B}}{q^2}\frac{1}{e^{\beta\omega}+1}\int \frac{p^4 dp\, d\cos\theta_p}{(2\pi)^3}\frac{1}{2E}\frac{e^{\beta E}}{(e^{\beta E}-1)^2}
$$
$$
\times\left(\left(\left(t_\zeta\theta - \frac{1}{2}t_\eta\sigma\right)+\frac{3}{2}t_\eta\sigma\cos^2\theta_p\right)\left(\frac{12}{f_\pi^2}q^2\mathrm{Im}\Pi_V(q^2)\right)\right.
$$
$$
-\frac{6}{f_\pi^2}(p-q)^2\mathrm{Im}\mathbf{\Pi}_A((p-q)^2 + q \to -q)
$$
$$
+\frac{8}{f_\pi^2}((p\cdot q)^2 - m_\pi^2 q^2)\mathrm{Im}\mathbf{\Pi}_V(q^2)\times\mathrm{Re}\Delta_R(p-q)
$$
$$
\left.+\, q \to -q\right). \tag{46}
$$

The total viscous hadronic rate for dilepton emission is (44) plus (46),

$$
\frac{d\mathbb{R}}{d^4q} = \frac{d\mathbb{R}_0}{d^4q} + \frac{d\mathbb{R}_1}{d^4q}. \tag{47}
$$

V. PARTONIC PHASE

At high temperature, the fluid is that of strongly coupled partoniclike constituents (sQGP). We will treat it in leading order as made of partonic constituents in the presence of soft gluonic fields. Typically, the soft gluons are magnetic (scale g^2T). The soft corrections will be estimated as operator insertions in leading dimensions as in Ref. [24]. A similar proposal using soft insertions for the electromagnetic emissivities was also suggested in Ref. [25]. With this in mind, and for the generic process $[p_i] \to [q_f] + \gamma$, the unordered Wightman function reads [18]

$$
-\,G_\mu^{\mu<}(q)
$$
$$
= \int\prod_i\frac{d^3p_i^{\mathrm{in}}}{(2\pi)^3 2E_i^{\mathrm{in}}}n(E_i^{\mathrm{in}})\prod_j\frac{d^3q_j^{\mathrm{out}}}{(2\pi)^3 2E_j^{\mathrm{out}}}(1\pm n(E_j^{\mathrm{out}}))
$$
$$
\times (2\pi)^4\delta\left(\sum_i p_i - \sum_j q_j - q\right)|\mathbf{M}_{i\to f+\gamma}|^2. \tag{48}
$$

The effects of the viscous corrections amount to additional contributions to the initial and final distribution functions. We now detail them for both dilepton and photon emissions.

A. Dileptons

We now seek to organize the dilepton emissivities in the nonperturbative partonic phase as

$$
\frac{d^3\mathbb{R}}{d^4q} = \frac{d^3\mathbb{R}_0^{Tp}}{d^4q} + \frac{d^3\mathbb{R}_1^{Vp}}{d^4q} + \frac{d^3\mathbb{R}_0^{Tn}}{d^4q} + \frac{d^3\mathbb{R}_1^{Vn}}{d^4q} \tag{49}
$$

with the first contribution $\mathbb{R}_0^{Tp}$ as the thermal perturbative rate, the second contribution $\mathbb{R}_1^{Vp}$ as the viscous perturbative correction, the third contribution $\mathbb{R}_0^{Tn}$ as the thermal and nonperturbative correction of leading mass dimension in the external fields, and finally the fourth contribution $\mathbb{R}_1^{Vp}$ as the viscous nonperturbative contribution in the leading mass dimension. The separation into perturbative (thermal and electric) and nonperturbative (magnetic) in the thermal state follows a similar reasoning for the use of the operator product expansion (OPE) expansion in the QCD sum rules for the hadronic correlators in the QCD vacuum. We now proceed to evaluate each of these contributions sequentially as (54), (61), (66), and (73), to be detailed below.

1. Thermal perturbative contribution

In leading order, the perturbative dilepton emissivity corresponds to an in state with a single $q\bar{q}$ as illustrated in Fig. 3, and its contribution to (48) is (omitting all charge factors)

$$
-G_\mu^{\mu<}(q) = \frac{q^2}{\pi|q|}\int_{\frac{q_0-|q|}{2}}^{\frac{q_0+|q|}{2}}dk f_\mu(k)f_{-\mu}(q_0 - k)
$$
$$
= n_B(q_0)\frac{q^2}{\pi|q|}\int_{q^-}^{q^+}(1 - f_\mu(k) - f_{-\mu}(q_0 - k))
$$
$$
= n_B(q_0)\frac{q^2}{\pi}n_B(q_0)\left(-1 + \frac{1}{\beta|q|}\ln\left(\frac{\mathrm{n}_\mu^-\mathrm{n}_{-\mu}^-}{\mathrm{n}_\mu^+\mathrm{n}_{-\mu}^+}\right)\right) \tag{50}
$$

We have defined the Fermi distributions at finite *chemical potential* μ as

$$
f_{\pm\mu}(q) = \frac{1}{e^{\beta(q_0\mp\mu)}+1} \tag{51}
$$

and their associated shifted distributions

$$
n_{\pm\mu}^\pm = \frac{1}{e^{\beta(q_0\pm|q|)/2\mp\beta\mu}+1}. \tag{52}
$$

The emergence of the Bose distribution $n_B = 1/(e^{\beta q_0} - 1)$ in (50) reflects on the KMS condition

$$
G_\mu^{\mu<}(q) = 2n_B(q_0)\mathrm{Im}iG_\mu^{\mu R}(q) \tag{53}
$$

at finite temperature and chemical potential μ in leading order. The finite chemical potential will be traded below for a complex chemical potential for a fixed color species and identified with the insertion of a soft A_4 contribution in the strongly coupled QGP [24,25]. For $\mu = 0$, Eq. (50), when

inserted in the general formula for dilepton emission (42) and upon restoring the color-flavor factor for partons $N_c \hat{e}_f^2 / 2$, yields the leading partonic dilepton rate

$$\frac{d\mathbb{R}_0^{Tp}}{d^4 q} = \frac{-\alpha^2 \mathbb{B}}{3\pi^3} \frac{1}{e^{\beta q_0} - 1}$$
$$\times \left(\frac{1}{4\pi} d_F \sum_f \hat{e}_f^2 \right) \left(1 + \frac{2}{\beta |q|} \ln \left(\frac{n^+}{n^-} \right) \right) \quad (54)$$

with $d_F = N_c$ the color dimension of the quark representation and $n^\pm \equiv n_{\pm 0}^\pm$. Here, $e\hat{e}_f$ is the electromagnetic charge of a quark of flavor f. In this order, the emission is isotropic.

2. Viscous perturbative contribution

The viscous corrections to the perturbative quark and gluon processes follow exactly along the general arguments we presented earlier in Secs. II and III. Specifically, for the fermionic Wightman functions

$$G_{\alpha\beta}^>(x) = + \langle \psi_\alpha(x) \bar{\psi}_\beta(0) \rangle$$
$$G_{\alpha\beta}^<(x) = - \langle \bar{\psi}_\beta(0) \psi_\alpha(x) \rangle, \quad (55)$$

the T_{ij} insertions amounts to additional contributions, and in leading order, we have

$$G^<(k) = -\frac{\pi \not{k}}{E} n(k_0)(\delta^- - \delta^+)$$
$$- t_H \partial_i \beta_j \frac{k^i k^j}{E} \frac{\pi \not{k}}{E} n(k_0)(1 - n(k_0))(\delta^- + \delta^+)$$
$$G^>(k) = +\frac{\pi \not{k}}{E} (1 - n)(\delta^- - \delta^+)$$
$$- t_H \partial_i \beta_j \frac{k^i k^j}{E} \frac{\pi \not{k}}{E} n(1 - n)(\delta^- + \delta^+) \quad (56)$$

with $\delta^\pm \equiv \delta(k_0 \mp k)$. In the real-time or double-line formalism, the total emission rate follows from the 12 Wightman function, where the effects of the T_{ij} insertions amount to modifying the *in-state* population by

$$n \to n + t_H \frac{k_i k_j}{E} \partial_i \beta_j n(1 \pm n) \quad (57)$$

and the *out-state* population by

$$n \to 1 - n - t_H \frac{k_i k_j}{E} \partial_i \beta_j n(1 \pm n). \quad (58)$$

With this in mind, the viscous corrections to the leading-order dilepton emission at finite chemical potential (50) is

$$+ t_H \partial_i \beta_j \frac{q^2}{\pi |q|} \int_{\frac{q_0 - |q|}{2}}^{\frac{q_0 + |q|}{2}} dk f_\mu (1 - f_\mu) f_{-\mu}(q_0 - k) \frac{k_i k_j}{k}$$
$$+ t_H \partial_i \beta_j \frac{q^2}{\pi |q|} \int_{\frac{q_0 - |q|}{2}}^{\frac{q_0 + |q|}{2}} dk f_{-\mu} (1 - f_{-\mu}) f_\mu(q_0 - k) \frac{k_i k_j}{k}, \quad (59)$$

which can be reorganized as follows:

$$t_H \partial_i \beta_j \frac{q^2}{\pi |q|}$$
$$\times \left(\frac{\delta_{ij} - \hat{q}_i \hat{q}_j}{2} \int_{\frac{q_0 - |q|}{2}}^{\frac{q_0 + |q|}{2}} dk k f_\mu (1 - f_\mu) f_{-\mu}(q_0 - k) \right.$$
$$+ \frac{3 \hat{q}_i \hat{q}_j - \delta_{ij}}{2} \int_{\frac{q_0 - |q|}{2}}^{\frac{q_0 + |q|}{2}} dk k f_\mu (1 - f_\mu) f_{-\mu}(q_0 - k)$$
$$\times \left. \left(\frac{q_0}{|q|} - 2 \frac{q_+ q_-}{|q| k} \right)^2 + \mu \to -\mu \right). \quad (60)$$

The $\mu = 0$ contribution in (60) yields the viscous perturbative contribution to the dilepton rate (54). More specifically, we have

$$\frac{d\mathbb{R}_1^{Vp}}{d^4 q} = \frac{\alpha^2 \mathbb{B}}{3\pi^3} \frac{1}{e^{\beta q_0} - 1} \times \left(\frac{1}{4\pi} d_F \sum_f \hat{e}_f^2 \right) \frac{2}{|q|}$$
$$\times \left(\frac{2 t_\zeta \theta - t_\eta \sigma}{2} \int_{\frac{q_0 - |q|}{2}}^{\frac{q_0 + |q|}{2}} dk k (1 - f - \tilde{f})(1 - f) \right.$$
$$+ \frac{3 t_\eta \sigma}{2} \int_{\frac{q_0 - |q|}{2}}^{\frac{q_0 + |q|}{2}} dk k (1 - f - \tilde{f})(1 - f)$$
$$\times \left. \left(\frac{q_0}{|q|} - 2 \frac{q_+ q_-}{|q| k} \right)^2 \right), \quad (61)$$

where we have defined the fermionic distributions $f \equiv f_0(k)$ and $\tilde{f} \equiv f_0(q_0 - k)$ for $\mu = 0$.

In Fig. 2, we show the ratio $d\mathbb{R}_1^{Vp} / d\mathbb{R}_0^{Tp}$ of the thermal viscous contribution (61) to the free thermal contribution (54), for dilepton emission at $q = (2\omega, \omega)$ as a function of $\beta\omega$, after setting $t_\zeta = t_\eta = \beta$ and $\theta = \sigma = 1$. The orange-dashed line is the shear ratio, while the blue-solid line is the bulk ratio. Again, the bulk contribution is larger than the shear contribution, and both are positive and increasing with $\beta\omega$.

3. Thermal nonperturbative contribution

The partonic phase near the transition temperature still carries soft gluons [24,25]. Their effects is to modify both the thermal and viscous rates. A way to assess these nonperturbative effects is to organize these modifications as power corrections through gluonic operators insertions of increasing dimension $\Delta = 2, 4$ in the JJ correlation function. In Fig. 3, we illustrate the leading soft gluonic insertions on the dilepton emissivities. Typically, these
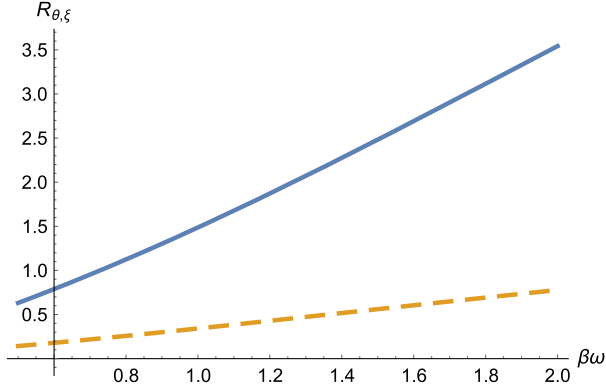
FIG. 2. Ratio $d\mathbb{R}_1^{Vp}/d\mathbb{R}_0^{Tp}$ for the thermal perturbative dilepton bulk contribution R_ζ (blue-solid curve) vs $\beta\omega$ and for the thermal perturbative shear dilepton contribution R_η (orange-dashed curve) vs $\beta\omega$ and $q = (2\omega, \omega)$. We have set the relaxation times $t_\zeta = t_\eta = \beta$ and fixed $\theta = \sigma = 1$.
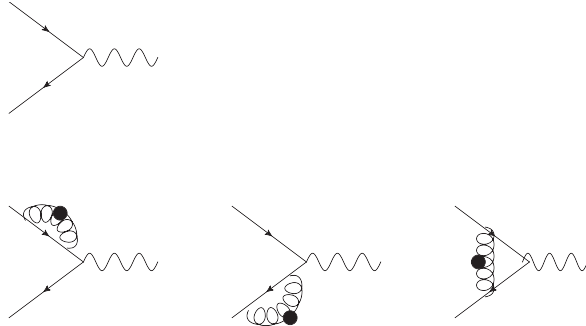

FIG. 3. Thermal dilepton emission including the leading perturbative term (top) and the leading soft and nonperturbative corrections (bottom). The blob refers to gluon insertions of leading dimensions $(gA_4)^2$, $(gE)^2$, and $(gB)^2$.

contributions are of the form $(gA_4)^2, (gE)^2, (gB)^2, \dots$ and of order $(g^2T)^\Delta$.

Since a constant gA_4 acts as an imaginary colored chemical potential on the quark line, the leading operator insertion $(gA_4)^2$ is readily obtained from the quadratic μ contribution stemming from the fermionic propagator at finite chemical potential, with the identification

$$\mu^2 \to -\langle (gA_4)^2 \rangle. \tag{62}$$

A proof of this is given in Appendix A using the background field method. With this in mind, the quadratic contribution stemming from (50) is

$$\ln\left(\frac{n_\mu^- n_{-\mu}^-}{n_\mu^+ n_{-\mu}^+}\right)$$
$$= +2\ln\left(\frac{n^-}{n^+}\right) + (\beta\mu)^2(n^+(1 - n^+) - n^-(1 - n^-))$$
$$+ \mathcal{O}(\mu^4), \tag{63}$$

which corrects the perturbative dilepton rate (54) by the nonperturbative contribution

$$-\frac{\alpha^2 \mathbb{B}}{3\pi^3}\frac{1}{e^{\beta q_0} - 1}\left(\frac{1}{4\pi}d_F\sum_f \hat{e}_f^2\right)\langle(gA_4)^2\rangle$$
$$\times\left(\frac{\beta}{|q|}\right)(n^+(1 - n^+) - n^-(1 - n^-)). \tag{64}$$

The effects of $(gE)^2$ and $(gB)^2$ can be calculated by general arguments using the background field method [24], as briefly recalled in the Appendix A. The net result can be understood using the simple substitution

$$\langle(gA_4)^2\rangle \to \langle(gA_4)^2\rangle - \frac{1}{6q^2}\langle(gE)^2\rangle + \frac{1}{3q^2}\langle(gB)^2\rangle, \tag{65}$$

a proof of which is given in Appendix A. The substitution can be understood as $(gqA_4) \sim gE \sim gB$. The factor of $\frac{1}{3}$ is from averaging over the vector orientations. The extra $-\frac{1}{2}$ in front of the electric contribution is due to the use of a fixed thermal frame and the fact that $(gE)^2 \sim -(gB)^2$ in Euclidean space. Hence, the final nonperturbative corrections to the dilepton rate (54) in leading operator insertions are

$$\frac{d\mathbb{R}_0^{Tn}}{d^4q} = \frac{\alpha^2\mathbb{B}}{3\pi^3}\frac{1}{e^{\beta q_0} - 1}\left(\frac{1}{4\pi}d_F\sum_f\hat{e}_f^2\right)$$
$$\times\left(-\langle(gA_4)^2\rangle + \frac{1}{6q^2}\langle(gE)^2\rangle - \frac{1}{3q^2}\langle(gB)^2\rangle\right)$$
$$\times\left(\frac{\beta}{|q|}\right)(n_+(1 - n_+) - n_-(1 - n_-)) \tag{66}$$

in agreement with the result in Ref. [24]. The typical values of the soft condensate insertions in (66) are discussed in Refs. [4,24].

4. Viscous nonperturbative contribution

The viscous and nonperturbative corrections to (61) can be obtained using the same reasoning developed above for the nonperturbative thermal corrections. For that, we expand the general result (60) to quadratic order in μ, by expanding the fermionic occupation number

$$f_\mu = f + \beta\mu f(1 - f) + \frac{1}{2}(\beta\mu)^2 f(1 - f)(1 - 2f) + \mathcal{O}(\mu^3). \tag{67}$$

Now, we use the identity

$$\int f_\mu(1 - f_\mu)f_{-\mu}(q_0 - k)[\dots]$$
$$= n_B(q_0)\int(1 - f_\mu - f_{-\mu}(q_0 - k))(1 - f_\mu)[\dots] \tag{68}$$

and expand the integrand in μ. The quadratic contribution reads

$$((1-f_\mu-\tilde{f}_{-\mu})(1-f_\mu)+(\mu\to-\mu))_{\mu^2}$$
$$=+2f(1-f)^2(3f-1)+f(1-f)(1-2f)(\tilde{f}-1)$$
$$+\tilde{f}(1-\tilde{f})(1-2\tilde{f})(f-1)-2f(1-f)\tilde{f}(1-\tilde{f}). \quad (69)$$

With the help of the identity

$$2f(1-f)^2(3f-1)$$
$$=(1+n_B(q_0))(1-\tilde{f}-f)(f(1-2f)+\tilde{f}(1-2\tilde{f}))$$
$$-2n_B(q_0)(1+n_B(q_0))(1-f-\tilde{f})^2, \quad (70)$$

The μ^2 correction to (59) is

$$(\beta\mu)^2 t_H \partial_i\beta_j \frac{q^2}{\pi|q|}$$
$$\times\left(\frac{\delta_{ij}-\hat{q}_i\hat{q}_j}{2}(n_B F_1 + n_B(1+n_B)F_2 + n_B^2(1+n_B)F_3)\right.$$
$$\left.+\frac{3\hat{q}_i\hat{q}_j-\delta_{ij}}{2}(n_B\tilde{F}_1 + n_B(1+n_B)\tilde{F}_2 + n_B^2(1+n_B)\tilde{F}_3)\right), \quad (71)$$

where we have defined

$$F_1=+2\int dkk f(1-f)^2(3f-1)$$
$$\tilde{F}_1=+2\int dkk f(1-f)^2(3f-1)\left(\frac{q_0}{|q|}-\frac{2q_+q_-}{|q|k}\right)^2$$
$$F_2=-\int dkk(1-\tilde{f}-f)(f(1-2f)+\tilde{f}(1-2\tilde{f}))$$
$$\tilde{F}_2=-\int dkk(1-\tilde{f}-f)(f(1-2f)+\tilde{f}(1-2\tilde{f}))$$
$$\times\left(\frac{q_0}{|q|}-\frac{2q_+q_-}{|q|k}\right)^2$$
$$F_3=-2\int dkk(1-\tilde{f}-f)^2$$
$$\tilde{F}_3=-2\int dkk(1-\tilde{f}-f)^2\left(\frac{q_0}{|q|}-\frac{2q_+q_-}{|q|k}\right)^2. \quad (72)$$

Using the operator substitutions (62)–(65) for μ^2 in (71) leads to the nonperturbative corrections to the viscous dilepton emission rate (61) in the form [$n_B \equiv n_B(q_0)$]

$$\frac{d\mathbb{R}_1^{Vn}}{d^4q}=\frac{\alpha^2\mathbb{B}}{3\pi^3 q^2}\frac{\beta^2}{e^{\beta q_0}-1}\left(\frac{1}{4\pi}d_F\sum_f\hat{e}_f^2\right)\frac{q^2}{\pi|q|}$$
$$\times\left(-\langle(gA_4)^2\rangle+\frac{1}{6q^2}\langle(gE)^2\rangle-\frac{1}{3q^2}\langle(gB)^2\rangle\right)$$
$$\times\left(\frac{2t_\zeta\theta-t_\eta\sigma}{2}(n_B F_1 + n_B(1+n_B)F_2 + n_B^2(1+n_B)F_3)\right.$$
$$\left.+\frac{3t_\eta\sigma}{2}(n_B\tilde{F}_1 + n_B(1+n_B)\tilde{F}_2 + n_B^2(1+n_B)\tilde{F}_3)\right). \quad (73)$$

B. Photons

Following the dilepton analysis, we now seek to organize the photon emissivities in the nonperturbative partonic phase as

$$\frac{xd^3\Gamma}{d^3k}=\frac{d^3\Gamma_0^{Tp}}{d^3k}+\frac{d^3\Gamma_1^{Vp}}{d^3k}+\frac{d^3\Gamma_0^{Tn}}{d^3k}+\frac{d^3\Gamma_1^{Vn}}{d^3k} \quad (74)$$

with the first contribution Γ_0^{Tp} as the thermal perturbative rate, the second contribution Γ_1^{Vp} as the viscous perturbative correction, the third contribution Γ_0^{Tn} as the thermal and nonperturbative correction of leading mass dimension in the external fields, and finally the fourth contribution Γ_1^{Vp} as the viscous nonperturbative contribution in leading mass dimension in the external fields. We now proceed to evaluate each of these contributions sequentially as (87), (96), (102), and (105), to be detailed below.

1. General

The photon analysis is more involved since the in state with $q\bar{q}$ is kinematically not allowed. The partonic photon
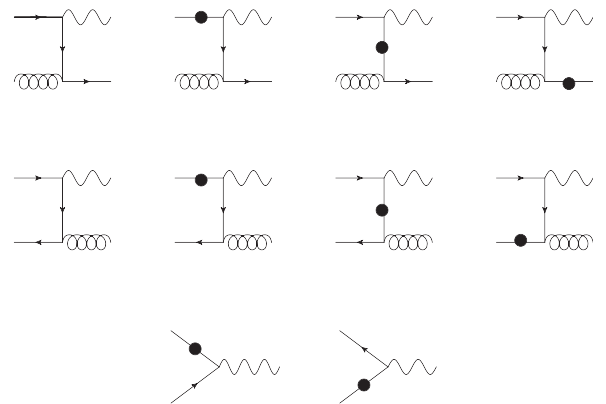

FIG. 4. Thermal photon emission including the leading perturbative term and the leading soft and nonperturbative corrections. The blob refers to gluon insertions of leading dimensions $(gA_4)^2$, $(gE)^2$, and $(gB)^2$. Soft vertex insertions as in Fig. 3 are also included but not shown. The last two contributions are not allowed without the soft insertions.

emission proceeds through 1) the Compton channel, with $qg \to \gamma q$ or $\bar{q}g \to \gamma \bar{q}$, and 2) the pair annihilation channel with $\bar{q}q \to g\gamma$, as illustrated in Fig. 4. Specifically, we have

$$G^<_{\text{compton}} = \frac{\mathbf{N}}{8(2\pi)^4 E} \int ds dt |M_c(s,t)|^2$$

$$\times \int dE_1 dE_2 f_\mu(E_1) f_g(E_2)(1 - f_\mu(E_1 + E_2 - E))$$

$$\times \frac{\theta(E_1 + E_2 - E)}{\sqrt{aE_1^2 + bE_1 + c}} + \mu \to -\mu \qquad (75)$$

with $E = \omega = k$ throughout, and

$$G^<_{\text{pair}} = \frac{\mathbf{N}}{8(2\pi)^4 E} \int ds dt |M_p(s,t)|^2$$

$$\times \int dE_1 dE_2 f_\mu(E_1) f_{-\mu}(E_2)(1 + f_g(E_1 + E_2 - E))$$

$$\times \frac{\theta(E_1 + E_2 - E)}{\sqrt{aE_1^2 + bE_1 + c}}. \qquad (76)$$

The leading perturbative contributions to the squared matrix elements are

$$\frac{|M_c(s,t,u)|^2}{16\pi^2} = -8\alpha\alpha_s \frac{u^2 + s^2}{us}$$

$$\frac{|M_p(s,t,u)|^2}{16\pi^2} = +8\alpha\alpha_s \frac{u^2 + t^2}{ut}, \qquad (77)$$

and the color-flavor factor is

$$\mathbf{N} = \frac{N_c^2 - 1}{2N_c} N_c \sum_f \hat{e}_f^2 \equiv C_F d_F \sum_f \hat{e}_f^2. \qquad (78)$$

The Mandelstam variables and the kinematical parameters a, b, and c are collectively defined as

$$s = (p_1 + p_2)^2$$
$$t = (p - p_1)^2$$
$$a = -(s + t)^2$$
$$b = 2(s + t)(Es - E_2 t)$$
$$c = st(s + t) - (Es + E_2 t)^2 \qquad (79)$$

with $s + t + u = 0$. The ranges of the integrations are $s \geq 0$ and $-s \leq t \leq 0$. However, the s integration is infrared sensitive, so the integration range will be modified to $s \geq m_T^2$ with the squared thermal quark mass $m_T^2 = \pi \alpha_s C_F / \beta^2$ as a regulator. These results are in agreement with those first reported in Ref. [26].

2. Thermal perturbative contribution

In this section, we will detail the approximations in the reduction of (75) and (76) in leading order, as they will be used for the viscous contributions as well. Following Ref. [26], we can unwind the integrations through the Boltzmann approximation

$$f_0(E_1) f_g(E_2) \sim e^{-\beta(E_1 + E_2)} \sim e^{-\beta E} \qquad (80)$$

in terms of which the integrand is typically of the form

$$\int dE_1 dE_2 f(E_1 + E_2 - E) \frac{\theta(E_1 + E_2 - E)}{\sqrt{aE_1^2 + bE_1 + c}}. \qquad (81)$$

After the change of variables $E_1 = x' + y$, $E_2 = x' - y$, this integral simplifies

$$2 \int dx' \int dy \frac{f(2x' - E)}{\sqrt{s^2(y - y_2)(y_1 - y)}} \qquad (82)$$

with the integration over y giving just $\frac{\pi}{s}$. From the constraint

$$2(E_1 + E_2 - E)E(1 - \cos\theta_{34}) = s, \qquad (83)$$

where $\cos\theta_{34} = \hat{p}_3 \cdot \hat{p}_4$, we find that $2x' - E = 2x \geq \frac{s}{8E}$, and (81) gives

$$\frac{2\pi}{s} \int_{\frac{s}{8E}}^{\infty} dx f(2x). \qquad (84)$$

For either distribution $f = \frac{1}{e^{\beta x} \pm 1}$, we obtain

$$\frac{\pi}{\beta s} \ln(1 \pm e^{-\frac{\beta s}{4E}})^{\pm 1}. \qquad (85)$$

The t integrations can be carried explicitly with the results

$$\int \frac{dt}{s} |M_c(s,t)|^2$$

$$= 128\pi^2 \alpha\alpha_s \left(\ln\left(\frac{s - m_T^2}{m_T^2}\right) + \frac{1}{2}\left(1 - \frac{2m_T^2}{s}\right) \right)$$

$$\times \int \frac{dt}{s} |M_p(s,t)|^2$$

$$= 256\pi^2 \alpha\alpha_s \left(\ln\left(\frac{s - m_T^2}{m_T^2}\right) - \left(1 - \frac{2m_T^2}{s}\right) \right). \qquad (86)$$

Again, the infrared cutoff satisfies $2m_T^2 \leq s$, $-s + m_T^2 \leq t \leq -m_T^2$. With the above in mind, the leading equilibrium photon emission from a perturbative QCD plasma associated to the Compton $qg \to q\gamma$ and pair creation $q\bar{q} \to \gamma g$ processes is [26]

$$\frac{d\Gamma_0^{Tp}}{d^3k} = \frac{\alpha\alpha_s}{\pi} \frac{1}{E\beta^2} \frac{1}{e^{\beta E} - 1}$$

$$\times \left(\frac{1}{4\pi} C_F d_F \sum_f \hat{e}_f^2\right)\left(\frac{1}{2}\ln\left(\frac{4E}{\beta m_T^2}\right) + \mathbf{C}\right). \qquad (87)$$

Here, **C** is a constant. The emission rate to this order is isotropic. In (87), the overall substitution

$$e^{-\beta E} \to \frac{1}{e^{\beta E} - 1} \qquad (88)$$

was made to recover the causal prefactor required by the KMS condition for the retarded process as in (53).

Finally, we remark that the perturbative photon rate (87) receives additional perturbative corrections to the same order in $\alpha\alpha_s$ through collinear bremsstrahlung [27]. This effect and its resummation will not be discussed here. Instead, we will focus on the potentially soft gluonic corrections that are also important near the transition temperature, as we now detail.

3. Viscous perturbative contributions

As we noted in the dilepton rates above, the viscous corrections in leading order correspond to the pertinent insertions of $k_i k_j$ on the partonic lines as given in (57)–(58). These gradient insertions break the isotropic character of the integrations with the typical integral structures

$$q_i q_j \int \cos^2\theta + \frac{(\delta_{ij} - q_i q_j)}{2} \int (1 - \cos^2\theta)$$

$$= q_i q_j \int \frac{3\cos^2\theta - 1}{2} + \delta_{ij} \int \frac{1 - \cos^2\theta}{2}, \qquad (89)$$

where the scattering angles are defined as

$$\cos\theta_1 = \frac{t + 2EE_1}{2EE_1}$$

$$\cos\theta_2 = \frac{u + 2EE_2}{2EE_2}$$

$$\cos\theta_3 = \frac{2(E_1 + E_2 - E)E - s}{2E(E_1 + E_2 - E)}. \qquad (90)$$

The angles $\theta_{1,2,3}$ refer to the angles between particles 1, 2, and 3 and γ flying along the z direction, in the process labeled as $1 + 2 \to 3 + \gamma$. To proceed, we now make two kinematical approximations to simplify the integration analyses to follow. The first is to follow (A2) and approximate the population factors by

$$f_{\pm\mu}(E_1)(1 - f_{\pm\mu}(E_1))f_g(E_2) \approx e^{-\beta(E_1 + E_2 \mp \mu)}$$

$$f_{\pm\mu}(E_1)(f_g)(1 + f_g) \approx e^{-\beta(E_1 + E_2 \mp \mu)}, \qquad (91)$$

and the second is to replace $E_{1,2}$ in $\cos(\theta_{1,2})$ by $E_{1,2} \approx (E_1 + E_2)/2$. These approximations will allow us to extract explicit estimates for the viscous perturbative and nonperturbative effects. They will be tested against realistic hydrodynamical evolution of the rates in the future. With this in mind, the viscous corrections to the Compton (75) and pair (76) are, respectively, given by

$$-G_c^< = t_H \partial_i \beta_j \left(\frac{\delta_{ij} - \hat{q}_i \hat{q}_j}{2} G_c^P + \frac{3\hat{q}_i \hat{q}_j - \delta_{ij}}{2} G_c^T\right)$$

$$-G_p^< = t_H \partial_i \beta_j \left(\frac{\delta_{ij} - \hat{q}_i \hat{q}_j}{2} G_p^P + \frac{3\hat{q}_i \hat{q}_j - \delta_{ij}}{2} G_p^T\right), \qquad (92)$$

where the upper labels P and T follow the separation into 1 and $\cos^2\theta$ in the decomposition in (89). The Compton kernels are

$$G_c^P \approx \frac{\mathbf{N}}{8(2\pi)^3 E} \frac{1}{e^{\beta(E-\mu)} - 1} \int \frac{dsdt}{s} |M_c(s,t)|^2$$

$$\times \int_{\frac{s}{8E}}^\infty dx \left(\frac{2x + E}{e^{\beta(2x-\mu)} + 1} - \frac{2xe^{\beta(2x-\mu)}}{(e^{\beta(2x-\mu)} + 1)^2}\right)$$

$$+ \mu \to -\mu$$

$$G_c^T \approx \frac{\mathbf{N}}{8(2\pi)^3 E} \frac{1}{e^{\beta(E-\mu)} - 1} \int \frac{dsdt}{s} |M_c(s,t)|^2$$

$$\times \int_{\frac{s}{8E}}^\infty dx \left(\frac{2x + E - \frac{s}{E} + \frac{t^2 + (s+t)^2}{8xE^2}}{e^{\frac{2x-\mu}{T}} + 1}\right.$$

$$\left. - \frac{2xe^{\beta(2x-\mu)}\left(1 - \frac{s}{4Ex}\right)^2}{(e^{\beta(2x-\mu)} + 1)^2}\right) + \mu \to -\mu, \qquad (93)$$

and the pair production kernels are

$$G_p^P \approx \frac{\mathbf{N}}{8(2\pi)^3 E} \frac{1}{e^{\beta E} - 1} \int \frac{dsdt}{s} |M_p(s,t)|^2$$

$$\times \int_{\frac{s}{8E}}^\infty dx \left(\frac{2x + E}{e^{\beta 2x} - 1} + \frac{2xe^{\beta 2x}}{(e^{\beta 2x} - 1)^2}\right)$$

$$G_p^T \approx \frac{\mathbf{N}}{8(2\pi)^3 E} \frac{1}{e^{\beta E} - 1} \int \frac{dsdt}{s} |M_p(s,t)|^2$$

$$\times \int_{\frac{s}{8E}}^\infty dx \left(\frac{2x + E - \frac{s}{E} + \frac{t^2 + (s+t)^2}{8xE^2}}{e^{\beta 2x} - 1} + \frac{2xe^{\beta 2x}\left(1 - \frac{s}{4Ex}\right)^2}{(e^{\beta 2x} - 1)^2}\right), \qquad (94)$$

which are independent of the chemical potential μ. In both kernels in (93) and (94), the substitution (88) was performed to recover the causal prefactor required by the KMS condition. In terms of the hydrodynamical times, Eq. (92) reads

$$-G_c^< = \left(\frac{2t_\zeta \theta - t_\eta \sigma}{2} G_c^P + \frac{3t_\eta \sigma}{2} G_c^T \right)$$

$$-G_p^< = \left(\frac{2t_\zeta \theta - t_\eta \sigma}{2} G_p^P + \frac{3t_\eta \sigma}{2} G_p^T \right), \qquad (95)$$

and the perturbative viscous correction to the photon rate takes the final form

$$\frac{d^3 \Gamma_1^{\mathrm{Vp}}}{d^3 k} = \frac{-1}{(2\pi)^3 2E} (G_c^< + G_p^<)_{\mu=0} \qquad (96)$$

after setting $\mu = 0$ in (93). In Appendix B, we make explicit the contributions to (96). The ratio of the leading shear and bulk thermal contributions in (96) to the leading thermal perturbative photon contribution (87) is found to be

$$R_\eta = \frac{d^3 \Gamma_{\mathrm{shear}}^{Vp}}{d^3 \Gamma_0^T} \approx \left(E + \frac{1}{\beta} \left(A_1 - 2A_2 - \frac{1}{3} - \frac{7\zeta_3}{\pi^2} \right) \right) t_\eta \sigma$$

$$R_\zeta = \frac{d^3 \Gamma_{\mathrm{bulk}}^{Vp}}{d^3 \Gamma_0^T} \approx \left(E + \frac{1}{\beta} \left(\frac{2}{3} + \frac{14\zeta_3}{\pi^2} \right) \right) t_\zeta \theta \qquad (97)$$

with $E = \omega = k_0$. Here, $A_{1,2}$ are functions of E defined in (B10), which asymptote zero at large E exponentially, and ζ_3 refers to the Riemann zeta function. In Fig. 5, we show the ratios (97) vs $\beta\omega$ with $\omega = E$, for $t_\zeta = t_\eta = \beta$ and fixed $\theta = \sigma = 1$. The thermal viscous corrections to the photon emissivities become linearly large at large $E = \omega \gg 1/\beta$. Since Eq. (97) were derived for large $E = \omega \gg 1/\beta$, the low $E = \omega \ll 1/\beta$ part of the curve receives additional corrections. Note that the constants contributions were dropped from both the perturbative and viscous rates at large $E = \omega \gg 1/\beta$.

4. Thermal nonperturbative contributions

To obtain the thermal nonperturbative corrections to the photon rates, we proceed as in the case of the dilepton rates
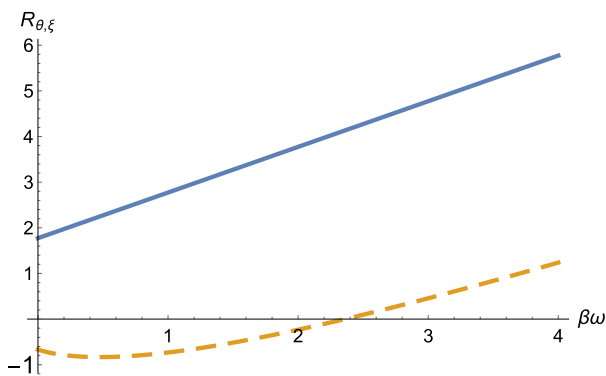

FIG. 5. Ratios (97) for the photon thermal bulk contribution R_ζ (blue-solid curve) vs $\beta\omega$, and for the photon thermal shear contribution R_η (orange-dashed curve) vs $\beta\omega$ and equal relaxation times $t_\zeta = t_\eta = \beta$ for fixed $\theta = \sigma = 1$.

above, by expanding (93) to order μ^2 and then trading μ^2 as in (62). With this in mind, we have

$$-G_c|_{\mu^2} = (\beta\mu)^2 (G_1 + G_2) \qquad (98)$$

with

$$G_1 = \frac{\mathbf{N}}{16(2\pi)^3 \beta E} n_B (1 + n_B)(1 + 2n_B)$$

$$\times \int \frac{ds\,dt}{s} |M_c(s,t)|^2 \ln(1 + e^{-\frac{s}{4E}})$$

$$G_2 = \frac{\mathbf{N}}{16(2\pi)^3 \beta E} n_B \int \frac{ds\,dt}{s} |M_c(s,t)|^2 \frac{e^{\frac{\beta s}{4}}}{(1 + e^{\frac{\beta s}{4}})^2}. \qquad (99)$$

The associated nonperturbative photon rate is

$$-\frac{\beta^2}{(2\pi)^3 2E} \langle (gA_4)^2 \rangle (G_1 + G_2)_{\mu=0}, \qquad (100)$$

which corresponds to the leading soft gluon insertion to the Compton process. We now note that, even though the perturbative annihilation process $q\bar{q} \to \gamma$ is kinematically forbidden, its counterpart in the presence of external fields (gE) and (gB) is not. This contribution can be obtained from the $\gamma^* \to q\bar{q}$ process in (66) after suitably multiplying by q^2 and then taking $q^2 \to 0$ to recover the photon point through the dilepton-photon identity

$$q_0 \frac{d^3 \Gamma}{d^3 q} = \frac{3\pi}{2\alpha \mathbb{B}} \lim_{q^2 \to 0} \left(q^2 \frac{d^4 \mathbb{R}}{d^4 q} \right). \qquad (101)$$

The outcome combined with (100) gives

$$\frac{d^3 \Gamma_0^{Tn}}{d^3 k} = \frac{\alpha}{2\pi^2 E} \frac{1}{e^{\beta E} - 1} \left(\frac{1}{4\pi} d_F \sum_f \hat{e}_f^2 \right)$$

$$\times \left(\frac{1}{6} \langle (gE)^2 \rangle - \frac{1}{3} \langle (gB)^2 \rangle \right)$$

$$\times \left(\frac{\beta}{|q|} \right) (n_+(1 - n_+) - n_-(1 - n_-)) \Bigg)$$

$$- \frac{\beta^2}{(2\pi)^3 2E} \langle (gA_4)^2 \rangle (G_1 + G_2)_{\mu=0}. \qquad (102)$$

The explicit forms of $G_{1,2}$ follow the same analysis detailed in Appendix B. This is our final result for the thermal and nonperturbative contributions for the photon emissivity, in leading mass dimensions.

5. Viscous nonperturbative contributions

The viscous nonperturbative contributions of the type $\langle (gA_4)^2 \rangle$ are readily obtained by expanding (93) in powers

of μ^2 and using the identification $\mu^2 \to -\langle (gA_4)^2 \rangle$ as we discussed above. We note that the μ dependence drops out of the pair production rate (94). More specifically, we have for the Compton contribution to second order in μ^2

$$G_c^P|_{\mu^2} = (\beta\mu)^2 G_3 \qquad G_c^T|_{\mu^2} = (\beta\mu)^2 G_4 \qquad (103)$$

with

$$G_3 = (1+n_B(E))(1+2n_B(E))G_c^P + \frac{N}{8(2\pi)^3 E} n_B(E) \int \frac{ds\,dt}{s} |M_c(s,t)|^2 \int_{\frac{s}{8E}}^{\infty} ((2x+E)f(1-f) - 2xf(1-f)(6f^2 - 6f + 1))$$

$$G_4 = (1+n_B(E))(1+2n_B(E))G_c^T + \frac{N}{8(2\pi)^3 E} n_B(E) \int \frac{ds\,dt}{s} |M_c(s,t)|^2 \int_{\frac{s}{8E}}^{\infty} \left(\left(2x + E - \frac{s}{E} + \frac{t^2 + (s+t)^2}{8xE^2} \right) f(1-f) \right.$$

$$\left. - 2x\left(1 - \frac{s}{4Ex}\right)^2 f(1-f)(6f^2 - 6f + 1) \right). \qquad (104)$$

Here, we have set $f = f(2x) = 1/(e^{\beta 2x} + 1)$. The nonperturbative viscous corrections to the photon rates are

$$\frac{d^3\Gamma_1^{Vn}}{d^3k} = \frac{-1}{(2\pi)^3 2E} G^<(E)$$

$$= + \frac{\alpha}{2\pi^2 E} \frac{1}{e^{\beta E} - 1} \left(\frac{1}{4\pi} d_F \sum_f \hat{e}_f^2 \right) \frac{\beta^2}{\pi E} \left(\frac{1}{6} \langle (gE)^2 \rangle - \frac{1}{3} \langle (gB)^2 \rangle \right)$$

$$\times \left(\frac{2t_\zeta \theta - t_\eta \sigma}{2} (n_B F_1 + n_B(1 + n_B) F_2 + n_B^2(1 + n_B) F_3) + \frac{3t_\eta \sigma}{2} (n_B \tilde{F}_1 + n_B(1 + n_B)\tilde{F}_2 + n_B^2(1 + n_B)\tilde{F}_3) \right)$$

$$- \frac{\beta^2}{(2\pi)^3 2E} \langle (gA_4)^2 \rangle \left(\frac{2t_\zeta \theta - t_\eta \sigma}{2} G_3 + \frac{3t_\eta \sigma}{2} G_4 \right). \qquad (105)$$

The first contribution stems again from the $q^2 \to 0$ of the nonperturbative viscous contribution for the $\gamma^* \to q\bar{q}$ rate in (73) using (101), and the last contribution follows from (103) after inserting it in (95) and combining it with (96) following the substitution $\mu^2 \to -\langle (gA_4)^2 \rangle$. Again, the explicit forms of $G_{3,4}$ follow the same analysis detailed in Appendix B. Equation (105) is our final result for the viscous and nonperturbative corrections to the photon rates in leading mass dimensions.

VI. CONCLUSION

We have provided a general framework for analyzing near-equilibrium hydrodynamical corrections to the photon and dilepton emissivities in QCD. Assuming that the emission times are short in comparison to the hydrodynamical evolution times, we have developed the rates by expanding the evolving fluid density matrix in derivatives of the fluid gradients. In leading order, the electromagnetic rates get corrected by bulk and shear viscous contributions in the form of Kubo-like response functions involving the energy-momentum tensor.

We have analyzed the viscous corrections in a hadronic fluid below the QCD transition temperature for both the photon and dilepton emissivities. A simple estimate of the photon rate using vector dominance in the chiral limit shows that the bulk viscosity corrections are much larger than the shear viscosity corrections for about all frequencies. The former are still sizable in the late stages of the hadronic evolution. These observations are interesting to check in a full hydrodynamical analysis of the photon emissivities at present colliders. Similar corrections were also shown to occur in the dilepton emission rates.

We have also analyzed the viscous corrections in a strongly coupled quark gluon plasma for temperatures higher than but close to the transition temperature, as probed by current colliders. The nonperturbative character of the sQGP is developed by correcting the thermal perturbative rates with soft gluonic insertions in the form of gluonic operators of increasing mass dimensions, in the spirit of the OPE expansion for the QCD vacuum correlation functions. The partonic thermal bulk viscous corrections to the dilepton and photon rates are observed to be more sizable than their shear counterparts with increasing dilepton and photon energies. As our calculations were carried out at finite chemical potential μ which was traded by an expansion with igA_4, they also provide for the viscous corrected electromagnetic rates at finite chemical potential as well.

The shortcomings of our analysis stem from our decoupling approximation that the hydrodynamical gradients decorrelate on time scales that are larger than the electromagnetic emission times and also our also assessment of

only the leading gradient corrections. To improve on this is more challenging technically, but straightforward conceptually. Without the viscous corrections, the hadronic rates and the partonic rates with the leading soft corrections are discussed in details in Refs. [4,28], and their implementation in a realistic hydrodynamical simulation is carried out in Ref. [28]. The rates are summarized in Appendix C for convenience by any hydrodynamical collaboration. The viscous corrections to the hadronic and partonic emissivities can and should be assessed in current analyses with hydrodynamical base evolution, in particular, their effects on the currently reported photon flow [6,15,28].

APPENDIX A: BACKGROUND FIELD ANALYSIS

In this Appendix, we briefly outline how to correct the Wightman function for the JJ correlator using the background field method as initially discussed in Ref. [24] and illustrated in Fig. 6. The soft gluon corrections are indicated by a blob. For the case of the leading $(gA_4)^2$ insertion discussed above, this construction relies directly on Feynman diagrams in the background field method, rather than the observation that A_4 plays the role of a colored chemical potential, and therefore can be traded by a real chemical potential as we discussed above. It also shows how the $(gE)^2$ and $(gB)^2$ corrections are obtained. Throughout this Appendix, the analysis is in Euclidean space, and we will set $A_4 = A_0$.

Using the Fock-Schwinger gauge for the background fields, we can explicitly rewrite the gauge fields as an expansion in increasing covariant derivatives of the field strengths,

$$A_0 = A_0 + x^i D_i A_0 + \cdots$$
$$A_i = x^j F_{ji} + \sum_{k=1} \frac{k+2}{k!} x^j x^{j_1} \cdots x^{j_k} D_{j_1} \cdots D_{j_k} F_{ji}. \quad (A1)$$
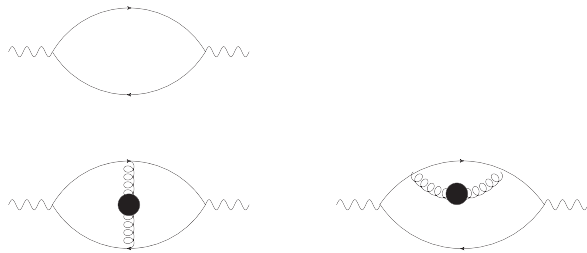

FIG. 6.   The thermal JJ correlation function in Euclidean space. The soft gluon insertions of the type $(gA_4)^2$, $(gE)^2$, $(gB)^2$ are indicated by a blob.

The fermion propagator in these external fields takes the form

$$S(q) = \int d^4 x e^{-iq \cdot x} \left\langle x \left| \frac{1}{-i\gamma \cdot D} \right| 0 \right\rangle. \quad (A2)$$

For simplicity, consider first the presence of a magnetic field B by limiting the external gauge field in D to A_i. Expanding (A2) to first order in B, we have

$$S_1(q) = -g \int \frac{d^4 q_1 d^4 q_2}{(2\pi)^4 (2\pi)^4} \frac{q_1 \cdot \gamma}{q_1^2} F_{ij} \gamma^j \frac{q_2 \cdot \gamma}{q_2^2} i \frac{\partial \delta^4(q_1 - q_2)}{\partial (q_1 - q_2)^i} e^{iq_1 \cdot x}; \quad (A3)$$

using $\frac{\partial \delta^4(q_1 - q_2)}{\partial (q_1 - q_2)^i} = -\frac{\partial \delta^4(q_1 - q_2)}{\partial q_2^i}$, we obtain

$$S_1(q) = -igS_0(q) F_{ij} \gamma^j \partial_i S_0(q)$$
$$S_0(q) = \frac{\not{q}}{q^2}. \quad (A4)$$

After a simple reduction, we have to first order in B

$$S_1[B] = -i \frac{g F_{ij}}{q^4} \gamma^i \not{q} \gamma^j. \quad (A5)$$

The second-order correction in B follows by expanding further in (A2), giving the contribution

$$-g^2 S_0(q_1) F_{ij} \gamma^j S_0(q_2) F_{kl} \gamma^l S_0(q_3)$$
$$\times \partial_{q_2 - q_3} \delta(q_2 - q_3) \partial_{q_1 - q_2} \delta(q_1 - q_2), \quad (A6)$$

which can be reduced by first partially integrating with respect to q_3, and then partially integrating with respect to q_2, to obtain

$$S_2[B] = -\frac{g^2 F_{ij} F_{kl}}{q^6} \not{q} \left(\gamma^j \gamma^k \gamma^i \gamma^l - \frac{4 q_i \gamma_j}{q^2} \gamma^k \not{q} \gamma^l \right). \quad (A7)$$

Color-spin averaging (A7) using

$$\langle F_{kl} F_{mn} \rangle = \frac{1}{8} \frac{1}{3} \langle B^2 \rangle (\delta_{km} \delta_{ln} - \delta_{kn} \delta_{lm})$$

leads to the B^2 correction to the fermionic propagator

$$\langle S_2[B] \rangle = \frac{2 \langle (gB)^2 \rangle}{3 q^6} \left(q_0 \gamma_0 - \frac{q_0^2}{q^2} \not{q} \right). \quad (A8)$$

Using similar arguments to those presented for the magnetic B, we can derive the corrections in A_0 and E to second order. The results are for the electric field

$$S_1[E] = -i\frac{gD_iA_0}{q^4}\left(\gamma^i \slashed{q}\gamma^0 - \frac{4q_0q_i}{q^2}\slashed{q}\right)$$

$$\langle S_2[E]\rangle = \frac{\langle(gE)^2\rangle}{8q^6}(\slashed{q}f_1 + q_0\gamma_0 f_2)$$

$$f_1 = \frac{1}{3} + \frac{28q_0^2}{3q^2} - \frac{16q_0^2|\vec{q}|^2}{q^4}$$

$$f_2 = -\frac{20}{3} + \frac{8|\vec{q}|^2}{3q^2} \tag{A9}$$

and for A_0

$$S_1[A_0] = -\frac{gA_0}{q^4}\slashed{q}\gamma_0\slashed{q}$$

$$S_2[A_0] = \frac{g^2A_0^2}{q^6}\slashed{q}\gamma_0\slashed{q}\gamma_0\slashed{q}. \tag{A10}$$

The leading magnetic correction to the Wightman function for the JJ correlator in Euclidean space is

$$\langle\Gamma_{\mu\mu}^E(q;[B])\rangle = e^2\langle(gB)^2\rangle(I_1 + I_2)$$

$$I_1 = -\frac{16}{3}\sum_{q_1+q_2=q}\frac{|\vec{q_1}|^2\omega_1\omega_2 - \omega_1^2\vec{q_1}\cdot\vec{q_2}}{q_1^8 q_2^2}$$

$$I_2 = -2\sum_{q_1+q_2=q}\frac{\omega_1\omega_2 + \frac{\vec{q_1}\cdot\vec{q_2}}{3}}{q_1^4 q_2^4} \tag{A11}$$

with $q = (\omega, \vec{q})$ and the shorthand notation

$$\sum_q \equiv \sum_{\omega_n = \pi T(2n+1)}\int\frac{d^3\vec{q}}{(2\pi)^3}.$$

The leading A_0 correction is

$$\langle\Gamma_{\mu\mu}^E(q;[A])\rangle = e^2\langle(gA_0)^2\rangle(I_3 + I_4)$$

$$I_3 = -8\sum_{q_1+q_2=q}\frac{\omega_1\omega_2(\omega_1^2 - 3|\vec{q_1}|^2) + (3\omega_1^2 - |\vec{q_1}|^2)\vec{q_1}\cdot\vec{q_2}}{q_1^6 q_2^2}$$

$$I_4 = -4\sum_{q_1+q_2=q}\frac{(\omega_1^2 - |\vec{q_1}|^2)(\omega_2^2 - |\vec{q_2}|^2) + 4\omega_1\omega_2\vec{q_1}\cdot\vec{q_2}}{q_1^4 q_2^4}. \tag{A12}$$

Here, I_4 follows from the soft insertion in the second contribution (bottom) of Fig. 6, and I_3 follows from the soft insertion in the first contribution (bottom) of Fig. 6.

If we set the external momentum $q = (q_0, \vec{0})$, then (A11) and (A12) can be reduced to

$$I_1 = \frac{32}{3}(2q_0 I_{31}^0 + I_{31}^{00} + q_0^2 I_{41}^{00} - I_{40}^{00})$$

$$I_2 = \frac{-1}{3}(2I_{12} - q_0^2 I_{22} + 4q_0 I_{22}^0 + 4I_{22}^{00})$$

$$I_3 = 4(-3q_0 I_{21}^0 + 4q_0 I_{31}^{000} + 2I_{21}^{00} - I_{11})$$

$$I_4 = 2(+2q_0^2 I_{22}^{00} - q_0^2 I_{12} + 2q_0 I_{12}^0 + I_{02}) \tag{A13}$$

with the following notation:

$$I_{mn}^{\mu_1...\mu_j} \equiv \sum_k\frac{k^{\mu_1}...k^{\mu_j}}{k^{2m}(k+q)^{2n}}. \tag{A14}$$

Some useful properties of these integrals can be found in Ref. [29]. In particular, we have the identity

$$2I_{12} - q_0^2 I_{22} = 4q_0 I_{22}^0 + 4I_{22}^{00}. \tag{A15}$$

The magnetic contribution I_2 in (A13) diverges in the infrared at zero temperature. This contribution can be reabsorbed in the definition of $m\bar{q}q$ at zero temperature. This will be assumed at finite temperature as well. Since the chiral condensate vanishes in the partonic phase, we will set this self energy–type contribution to zero. The same will be assumed for the analog electric contribution. With this in mind, the electric and magnetic contributions following from the soft gluon insertions contribute to the JJ correlator as

$$\langle\Gamma_{\mu\mu}^E(q;[E,B])\rangle = -4e^2\langle(gE)^2\rangle(2I_{12} - q_0^2 I_{22})$$

$$+ \frac{4e^2}{3}(\langle(gE)^2\rangle + \langle(gB)^2\rangle)$$

$$\times (2I_{12} - q_0^2 I_{22} + 4q_0 I_{22}^0 + 4I_{22}^{00}). \tag{A16}$$

The asymmetry between the electric and magnetic field is due to the breaking of Lorentz invariance introduced by the heat bath. The Matsubara summation in the I integrals reduces to a zero temperature plus a finite temperature part through the use of

$$\sum_{\omega_n=\pi T(2n+1)} \beta F(\omega_n) = \int_{-i\infty+i0}^{+i\infty+i0} \frac{dz}{2i\pi} \left(\frac{1}{2}-f(z)\right)(F(z)+F(-z)) \tag{A17}$$

with $f(z)$ a thermal Fermi distribution. The analytical continuation of the Euclidean correlator to its Minkowski counterpart follows through the discontinuity

$$\Gamma_\mu^{\mu<}(\omega) = \frac{1}{i(e^{\beta\omega}-1)} \text{Disc}\Gamma_{\mu\mu}^E(q_0 \to -i(\omega \pm i\epsilon)). \tag{A18}$$

The results for the $(gA_0)^2$ insertion are in complete agreement with those obtained using a chemical potential and then the substitution (62). The results for the $(gE)^2$, $(gB)^2$ insertions correspond to the substitution (65).

APPENDIX B: LEADING THERMAL VISCOUS PHOTON CORRECTION

In this Appendix, we detail the calculations leading to (97). We start by performing the integrals

$$\int \frac{dt}{s}(t^2+(s+t)^2)|M_c(s,t)|^2 = 128\pi^2\alpha\alpha_s \times \left(-\frac{2m_T^6}{3s}+m_T^4+m_T^2 s-\frac{2s^2}{3}+s^2\ln\left(\frac{s-m_T^2}{m_T^2}\right)\right)$$

$$\int \frac{dt}{s}(t^2+(s+t)^2)|M_p(s,t)|^2 = 128\pi^2\alpha\alpha_s \times \left(\frac{8m_T^6}{3s}-4m_T^4+8m_T^2 s-\frac{10s^2}{3}+2s^2\ln\left(\frac{s-m_T^2}{m_T^2}\right)\right). \tag{B1}$$

Much like the leading perturbative thermal contribution (87), the viscous thermal contributions are also infrared sensitive. The leading singularities are logarithmic. For the Compton G_c and the pair G_p amplitudes, they are

$$G_c^P \approx \frac{\mathbf{N}}{8(2\pi)^3\beta E}\frac{128\pi^2\alpha\alpha_s}{e^{\beta E}-1}\int_{2m_T^2}^\infty ds \ln\left(\frac{s-m_T^2}{m_T^2}\right)\sum_{n=1}^\infty \frac{(-1)^{n+1}e^{-\frac{ns\beta}{4E}}}{n}\left(E-\frac{1}{\beta}\left(1-\frac{1}{n}\right)\left(1+\frac{ns\beta}{4E}\right)\right)$$

$$G_c^T \approx \frac{\mathbf{N}}{4(2\pi)^3\beta E}\frac{128\pi^2\alpha\alpha_s}{e^{\beta E}-1}\int_{2m_T^2}^\infty ds \ln\left(\frac{s-m_T^2}{m_T^2}\right)\sum_{n=1}^\infty \frac{(-1)^{n+1}e^{-\frac{ns}{4ET}}}{2n}\left(E-\frac{1}{\beta}\left(1-\frac{1}{n}\right)\left(1+\frac{ns\beta}{4E}\right)+\frac{s}{E}(n-1)\right)$$

$$+ \int_{\frac{s}{8E}}^\infty dx(-1)^{n+1}e^{-2n\beta x}\left(\frac{s^2}{4E^2(x+\frac{E}{2})}-n\frac{s^2}{8E^2 x}\right) \tag{B2}$$

and

$$G_p^P \approx \frac{\mathbf{N}}{8(2\pi)^3\beta E}\frac{128\pi^2\alpha\alpha_s}{e^{\beta E}-1}\int_{2m_T^2}^\infty ds \ln\left(\frac{s-m_T^2}{m_T^2}\right)\sum_{n=1}^\infty \frac{e^{-\frac{ns\beta}{4E}}}{n}\left(E+\frac{1}{\beta}\left(1+\frac{1}{n}\right)\left(1+\frac{ns\beta}{4E}\right)\right)$$

$$G_p^T \approx \frac{\mathbf{N}}{4(2\pi)^3\beta E}\frac{128\pi^2\alpha\alpha_s}{e^{\beta E}-1}\int_{2m_T^2}^\infty ds \ln\left(\frac{s-m_T^2}{m_T^2}\right)\sum_{n=1}^\infty \frac{e^{-\frac{ns\beta}{4E}}}{2n}\left(E+\frac{1}{\beta}\left(1+\frac{1}{n}\right)\left(1+\frac{ns\beta}{4E}\right)-\frac{s}{E}(n+1)\right)$$

$$+ \int_{\frac{s}{8E}}^\infty dx e^{-2n\beta x}\left(\frac{s^2}{4E^2(x+\frac{E}{2})}+n\frac{s^2}{8E^2 x}\right). \tag{B3}$$

For a small infrared cutoff m_T, we now define the useful integrals

$$\int_{2m_T^2} ds s^k \ln\left(\frac{s-m_T^2}{m_T^2}\right)e^{-\frac{ns\beta}{4E}} = k!\left(\frac{4E}{n\beta}\right)^{k+1}\ln\left(\frac{4E}{\beta m_T^2}\right) + \mathbb{C} \tag{B4}$$

and

$$\int_{2m_T^2} ds s^k \ln\left(\frac{s-m_T^2}{m_T^2}\right)\int_{\frac{s}{8E}} dx\frac{e^{-2n\beta x}}{x+a} = k!\ln\left(\frac{4E}{\beta m_T^2}\right)\int_1^\infty \left(\frac{4E}{un\beta}\right)^{k+1}\frac{e^{-2n\beta a(u-1)}}{u}du + \mathbb{C}. \tag{B5}$$

Collecting the above results yields for the Compton and pair amplitudes

$$G_c^P = \frac{\mathbf{N}}{2(2\pi)^3\beta^2} \frac{128\pi^2\alpha\alpha_s}{e^{\beta E}-1} \left(\ln\left(\frac{4E}{\beta m_T^2}\right) \sum_{n=1} \frac{(-1)^{n-1}}{n^2} \left(E - \frac{2}{\beta}\left(1-\frac{1}{n}\right)\right) + \mathbf{C}_1 \right)$$

$$G_c^T = \frac{\mathbf{N}}{2(2\pi)^3\beta^2} \frac{128\pi^2\alpha\alpha_s}{e^{\beta E}-1} \left(\ln\left(\frac{4E}{\beta m_T^2}\right) \left(\sum_{n=1} \frac{(-1)^{n-1}}{n^2} \left(E + \frac{2}{\beta}\left(1-\frac{1}{n}\right) + \frac{8}{n\beta}\left(I_4\left(n,\frac{E}{2}\right) - \frac{n}{2}I_4(n,0)\right)\right) \right) \right) + \mathbf{C}_2 \right) \quad \text{(B6)}$$

and

$$G_p^P = \frac{\mathbf{N}}{2(2\pi)^3\beta^2} \frac{128\pi^2\alpha\alpha_s}{e^{\beta E}-1} \left(\ln\left(\frac{4E}{\beta m_T^2}\right) \sum_{n=1} \frac{1}{n^2} \left(E + \frac{2}{\beta}\left(1+\frac{1}{n}\right)\right) + \mathbf{C}_3 \right)$$

$$G_p^T = \frac{\mathbf{N}}{2(2\pi)^3\beta^2} \frac{128\pi^2\alpha\alpha_s}{e^{\beta E}-1} \left(\ln\left(\frac{4E}{\beta m_T^2}\right) \left(\times \sum_{n=1} \frac{1}{n^2} \left(\left(E - \frac{2}{\beta}\left(1+\frac{1}{n}\right)\right) + \frac{8}{n\beta}\left(I_4\left(n,\frac{E}{2}\right) + \frac{n}{2}I_4(n,0)\right)\right) \right) \right) + \mathbf{C}_2 \right), \quad \text{(B7)}$$

where we have defined

$$I_k(n,a) = \int_1^\infty \frac{e^{-2n\beta a(u-1)}}{u^k} \, du$$

$$I_k(n,0) = \frac{1}{k+1}. \quad \text{(B8)}$$

Here, $\mathbf{C}_{1,2,3,4}$ are constants. After further simplifications, we finally obtain

$$G_c^P = \frac{2\pi\alpha\alpha_s\mathbf{N}}{3\beta^2(e^{\beta E}-1)} \left(E - \frac{2}{\beta}\left(1 - \frac{9\zeta_3}{\pi^2}\right)\right) \ln\left(\frac{4E}{\beta m_T^2}\right)$$

$$G_p^P = \frac{4\pi\alpha\alpha_s\mathbf{N}}{3\beta^2(e^{\beta E}-1)} \left(E + \frac{2}{\beta}\left(1 + \frac{6\zeta_3}{\pi^2}\right)\right) \ln\left(\frac{4E}{\beta m_T^2}\right)$$

$$G_c^T = \frac{2\pi\alpha\alpha_s\mathbf{N}}{3\beta^2(e^{\beta E}-1)} \left(E + \frac{2}{\beta}A_1\right) \ln\left(\frac{4E}{\beta m_T^2}\right)$$

$$G_p^T = \frac{2\pi\alpha\alpha_s\mathbf{N}}{3\beta^2(e^{\beta E}-1)} \left(E - \frac{2}{\beta}A_2\right) \ln\left(\frac{4E}{\beta m_T^2}\right) \quad \text{(B9)}$$

with the E-dependent functions

$$A_1 = 1 - \frac{9\zeta_3}{\pi^2} - \frac{48}{\pi^2} \sum_{n=1} \frac{(-1)^n}{n^3} \left(I_4\left(n,\frac{E}{2}\right) - \frac{n}{2}I_4(n,0)\right)$$

$$A_2 = 1 + \frac{6\zeta_3}{\pi^2} - \frac{24}{\pi^2} \sum_{n=1} \frac{1}{n^3} \left(I_4\left(n,\frac{E}{2}\right) + \frac{n}{2}I_4(n,0)\right). \quad \text{(B10)}$$

Here, $\zeta_3 \equiv \zeta(3) \approx 1.202$ refers to the Riemann zeta function. Throughout, $\mathbf{N}$ is given in (78).

APPENDIX C: FORMULA SUMMARY

Here, we summarize our pertinent results for the viscous corrections for the electromagnetic emissivities, which could be used in hydrodynamical calculations:

(1) *Viscous photon hadronic rates*: Equation (32), which is equal to (30) plus (31).
(2) *Viscous dilepton hadronic rates*: Equation (47), which is equal to (44) plus (46).
(3) *Viscous dilepton hadronic rates*: Equation (49), which is equal to (54) plus (61) plus (66) plus (73).
(4) *Viscous photon partonic rates*: Equation (74), which is equal to (87) plus (96) plus (102) plus (105).

[1] U. Heinz and R. Snellings, Annu. Rev. Nucl. Part. Sci. **63**, 123 (2013).
[2] M. Luzum and H. Petersen, J. Phys. G **41**, 063102 (2014).
[3] D. A. Teaney, arXiv:0905.2433.
[4] C.-H. Lee and I. Zahed, Phys. Rev. C **90**, 025204 (2014).
[5] J. F. Paquet, C. Shen, G. S. Denicol, M. Luzum, B. Schenke, S. Jeon, and C. Gale, Phys. Rev. C **93**, 044906 (2016).
[6] H. van Hees, C. Gale, and R. Rapp, Phys. Rev. C **84**, 054906 (2011); R. Rapp, H. van Hees, and M. He, Nucl. Phys. **A931**, 696 (2014).
[7] S. S. Adler et al. (PHENIX Collaboration), Phys. Rev. Lett. **91**, 182301 (2003).
[8] A. Adare et al. (PHENIX Collaboration), Phys. Rev. Lett. **109**, 122302 (2012).
[9] A. Adare et al. (PHENIX Collaboration), Phys. Rev. C **94**, 064901 (2016).
[10] ALICE Collaboration, Phys. Lett. B **719**, 18 (2013).

[11] D. Lohner (ALICE Collaboration), J. Phys. Conf. Ser. 446, 012028 (2013).

[12] S. Chatrchyan et al. (CMS Collaboration), Phys. Rev. C 87, 014902 (2013).

[13] S. Chatrchyan et al. (CMS Collaboration), Phys. Rev. C 89, 044906 (2014).

[14] P. Kovtun, D. T. Son, and A. O. Starinets, Phys. Rev. Lett. 94, 111601 (2005).

[15] K. Dusling, arXiv:0901.2027; K. Dusling, Nucl. Phys. A839, 70 (2010); K. Dusling, G. D. Moore, and D. Teaney, Phys. Rev. C 81, 034907 (2010); M. Dion, J. F. Paquet, B. Schenke, C. Young, S. Jeon, and C. Gale, Phys. Rev. C 84, 064901 (2011); S. Mitra, P. Mohanty, S. Sarkar, and J. e. Alam, arXiv:1107.2500; C. Shen, U. W. Heinz, J. F. Paquet, I. Kozlov, and C. Gale, Phys. Rev. C 91, 024908 (2015); C. Shen, J. F. Paquet, U. Heinz, and C. Gale, Phys. Rev. C 91, 014908 (2015); J. F. Paquet, C. Shen, G. S. Denicol, M. Luzum, B. Schenke, S. Jeon, and C. Gale, Phys. Rev. C 93, 044906 (2016).

[16] K. A. Mamo and H. U. Yee, Phys. Rev. D 91, 086011 (2015).

[17] R. Baier, S. A. Stricker, O. Taanila, and A. Vuorinen, Phys. Rev. D 86, 081901 (2012).

[18] L. D. McLerran and T. Toimela, Phys. Rev. D 31, 545 (1985).

[19] T. Hayata, Y. Hidaka, T. Noumi, and M. Hongo, Phys. Rev. D 92, 065008 (2015); M. Buzzegoli, E. Grossi, and F. Becattini, J. High Energy Phys. 10 (2017) 091.

[20] J. V. Steele, H. Yamagishi, and I. Zahed, Phys. Lett. B 384, 255 (1996).

[21] H. Yamagishi and I. Zahed, Ann. Phys. (N.Y.) 247, 292 (1996).

[22] J. V. Steele, H. Yamagishi, and I. Zahed, Phys. Lett. B 384, 255 (1996); C. H. Lee and I. Zahed, Phys. Rev. C 90, 025204 (2014).

[23] C. Gale and J. I. Kapusta, Phys. Rev. C 35, 2107 (1987); C. Gale and J. I. Kapusta, Nucl. Phys. B357, 65 (1991); R. Rapp and J. Wambach, Adv. Nucl. Phys. 25, 1 (2000); G. Vujanovic, J. F. Paquet, G. S. Denicol, M. Luzum, S. Jeon, and C. Gale, Phys. Rev. C 94, 014904 (2016); R. Rapp and H. van Hees, Eur. Phys. J. A 52, 257 (2016).

[24] T. H. Hansson and I. Zahed, QCD Sum Rules At High Temperature, PRINT-90-0339 (STONY-BROOK); C. H. Lee, J. Wirstam, I. Zahed, and T. H. Hansson, Phys. Lett. B 448, 168 (1999).

[25] Y. Hidaka, S. Lin, R. D. Pisarski, and D. Satow, J. High Energy Phys. 10 (2015) 005.

[26] J. I. Kapusta, P. Lichard, and D. Seibert, Phys. Rev. D 44, 2774 (1991); Phys. Rev. D 47, 4171(E) (1993); R. Baier, H. Nakkagawa, A. Niegawa, and K. Redlich, Z. Phys. C 53, 433 (1992);

[27] P. B. Arnold, G. D. Moore, and L. G. Yaffe, J. High Energy Phys. 06 (2002) 030.

[28] Y. M. Kim, C. H. Lee, D. Teaney, and I. Zahed, Phys. Rev. C 96, 015201 (2017).

[29] T. H. Hansson and I. Zahed, Nucl. Phys. B292, 725 (1987).